



# Numerical investigation of the effect of rectangular and semicircular cavities filled with phase change materials installed on the solar wall

Jawed Mustafa<sup>1</sup> · Saeed Alqaed<sup>1</sup> · Fahad Awjah Almehmadi<sup>2</sup> · Shahid Husain<sup>3</sup> · Basharat Jamil<sup>4</sup> · Mohsen Sharifpur<sup>5,6</sup>

Received: 2 January 2023 / Accepted: 10 June 2023  
© The Author(s) 2023

## Abstract

The use of alternative energy sources, particularly solar energy, in buildings is rising and spreading around the globe. In this paper, a solar wall is analyzed using a numerical method. On the wall, a number of obstacles are placed in two shapes, rectangular (REC) and semicircular (SEC). The cavities are filled with organic phase-change materials. This study was performed in 7 h in the absence of solar radiation on the wall for different dimensions of obstacles in 5 different modes. Various temperatures have been investigated, including exhaust air temperature (TAR), Trombe wall temperature (TWL), and mean volume % of molten PCM in cavities. COMSOL software is used to carry out this numerical study. The results of this study showed that the use of SECs compared to RECs causes the TWL to be higher. In the most extreme case, at a 16 cm aspect ratio, the use of SECs gives a 2.1 °C increase in TWL relative to the REC one. The outlet TAR is also increased by the usage of SECs. The use of larger dimensions of the cavities has increased the TAR leaving the wall so that the TAR after 7 h of the absence of solar radiation, in the most significant case of SECs, was more than 295.5 K. The use of SECs also increases the PCM freezing time. In the largest case of cavities, using SECs increases the freezing time by 15 min compared to RECs.

**Keywords** Solar energy · Building · Numerical method · Phase change materials

## Introduction

The extreme dependence of industrial societies on energy resources, especially fossil fuels, and their increasing consumption have caused their depletion. Fossil fuels such as oil and coal are finite and take a long time to

regenerate. They produce large amounts of various toxic gases each year. Carbon dioxide, which is the most important gas produced by petroleum products, even natural gas, which is the cleanest type of fossil fuel, is a non-toxic gas; however, its greenhouse type is very dangerous that destroys the ozone layer (Ascione, Bianco et al. 2021, Yang, Wang et al. 2021). Burning petroleum products causes harmful gases to release, resulting in

Responsible Editor: Philippe Garrigues

✉ Mohsen Sharifpur  
mohsen.sharifpur@up.ac.za

Saeed Alqaed  
saalqaed@nu.edu.sa

Fahad Awjah Almehmadi  
falmehmadi@ksu.edu.sa

Shahid Husain  
shahidhusain@zhcet.ac.in

Basharat Jamil  
jamil.basharat@imdea.org

<sup>1</sup> Mechanical Engineering Department, College of Engineering, Najran University, P.O. Box (1988), Najran 61441, Saudi Arabia

<sup>2</sup> Department of Applied Mechanical Engineering, College of Applied Engineering, Muzahimiyah Branch, King Saud University, P.O. Box 800, Riyadh 11421, Saudi Arabia

<sup>3</sup> Department of Mechanical Engineering, Zakir Husain College of Engineering and Technology, Aligarh Muslim University, Aligarh 202002, India

<sup>4</sup> High Temperature Processes Unit, IMDEA Energy Institute, Av. Ramón de La Sagra, 3, Móstoles, 28935 Madrid, Spain

<sup>5</sup> Department of Mechanical and Aeronautical Engineering, University of Pretoria, Pretoria, South Africa

<sup>6</sup> Department of Medical Research, China Medical University Hospital, China Medical University, Taichung, Taiwan

**Fig. 1** Schematic of the studied wall with two types of SECs and RECs

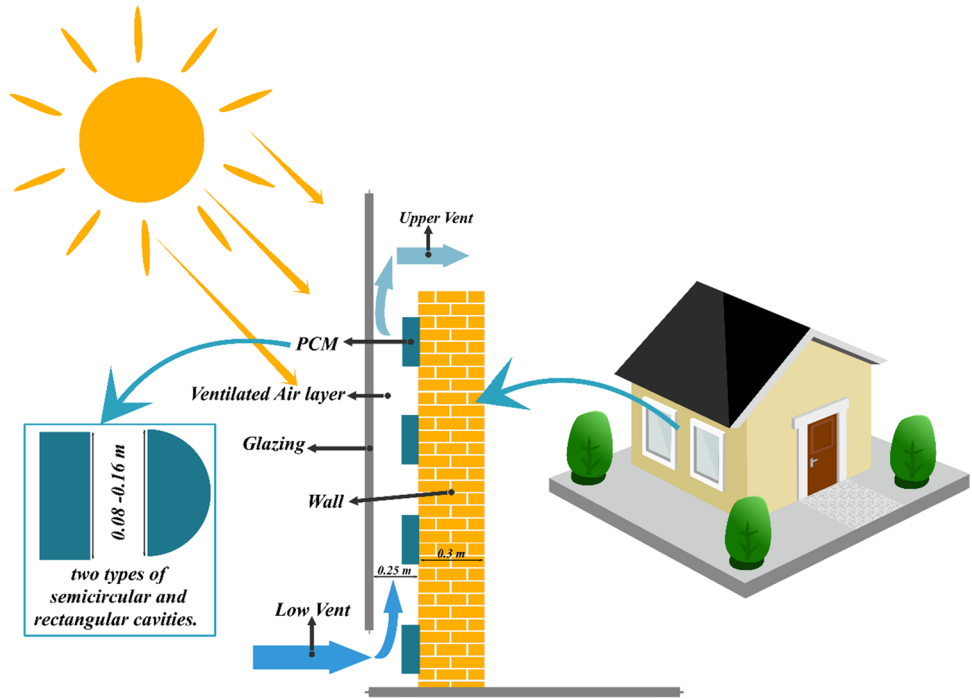


**Table 1** Thermo-physical properties of gallium

Density (kg/m <sup>3</sup> )	Specific heat (kJ/kg K)	Viscosity (kg/m/s *10 <sup>-3</sup> )	Thermal conductivity (W/m.k)	Melting point (K)
6094.7	397.6	1.75	33.6767	302.93

Altnji et al. 2021, Aghakhani and Afrand 2022). By using renewable energy, the environmental problems resulting from the consumption of fossil fuels and the amount of air pollution will be reduced, and saving on the consumption of fossil fuels (non-renewable) will be enhanced (Biwole, Eclache et al. 2013, Al-Abidi, Mat

the production of acid rain that has destructive effects on living organisms, forests, and even building materials. Clean energies do not have such negative effects on the environment (Mustafa, Alqaed et al. 2021, Xiong,

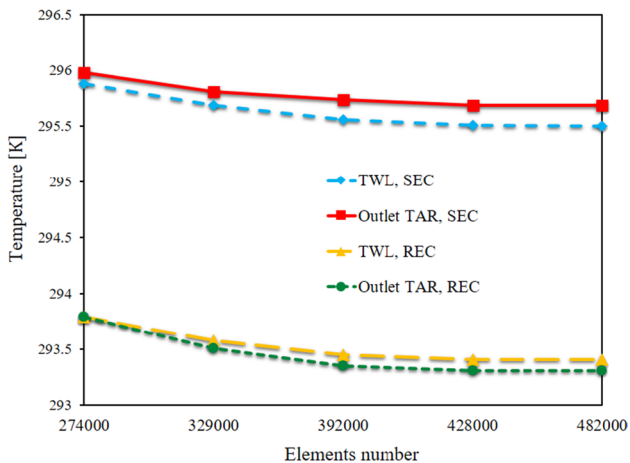


**Fig. 2** The effect of geometric meshing quality on TWL and outlet TAR in 16 cm aspect ratio for SEC and RECs

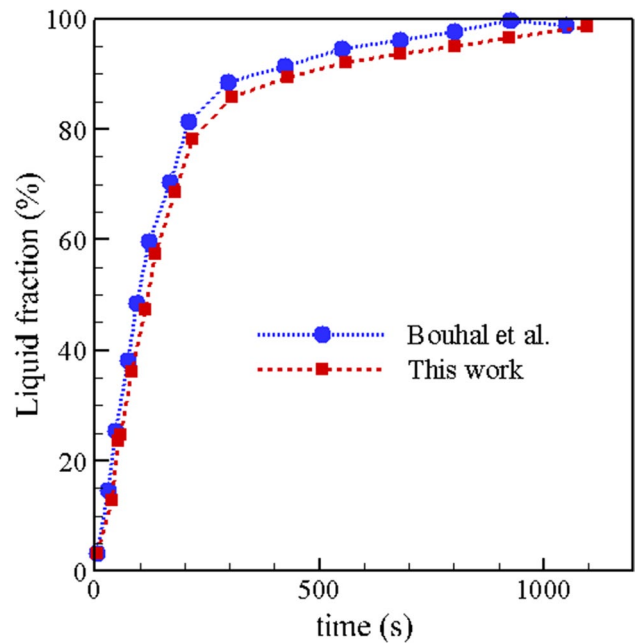


**Fig. 3** Comparison of melt PCM between the present work and Bouhal et al. (2018)

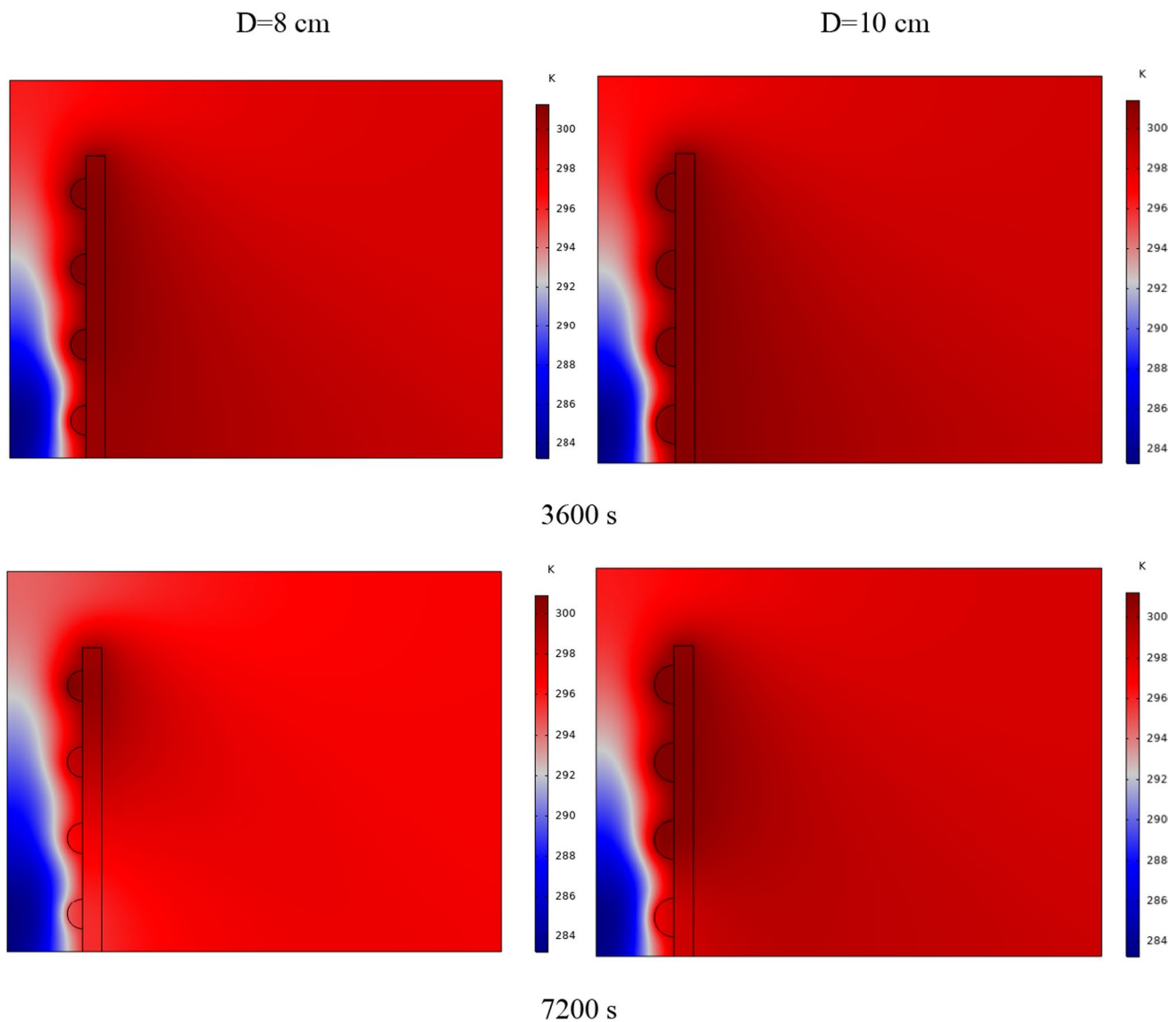


**Fig. 4** Temperature meter on the wall from 1 to 7 h for (D) 8 to 16 cm for SECs

et al. 2014, Barbosa and Ip 2014). Renewable energy is energy that can be returned to nature. Renewable energy sources are stable sources and can be used many times. Renewable energy sources include biomass, water, geothermal, solar, wind, and marine (Karthick, Suresh et al. 2019, Parsa, Yazdani et al. 2022). One of the most important sources of renewable energy is solar, which

has attracted the attention of many researchers for a long time. Solar energy is free and can be found worldwide (Aberoumand, Ghamari et al., 2018, Amjad, Jin et al., 2018, Mahdi, Lohrasbi et al., 2019). This kind of energy could be utilized in different ways, e.g. in buildings. Buildings require energy for heating and cooling so that people can live comfortably in them (Hu, He et al. 2017,

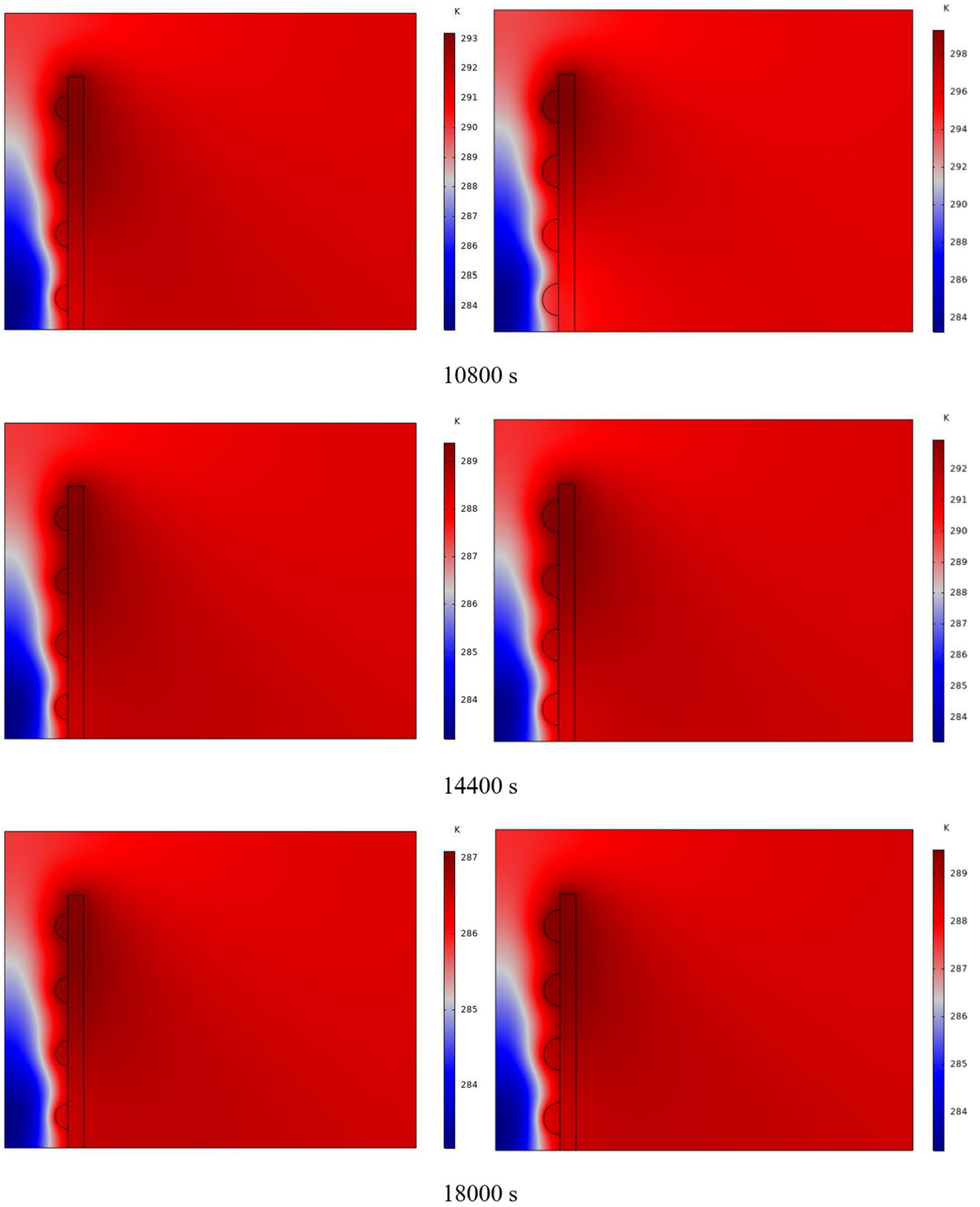


Fig. 4 (continued)

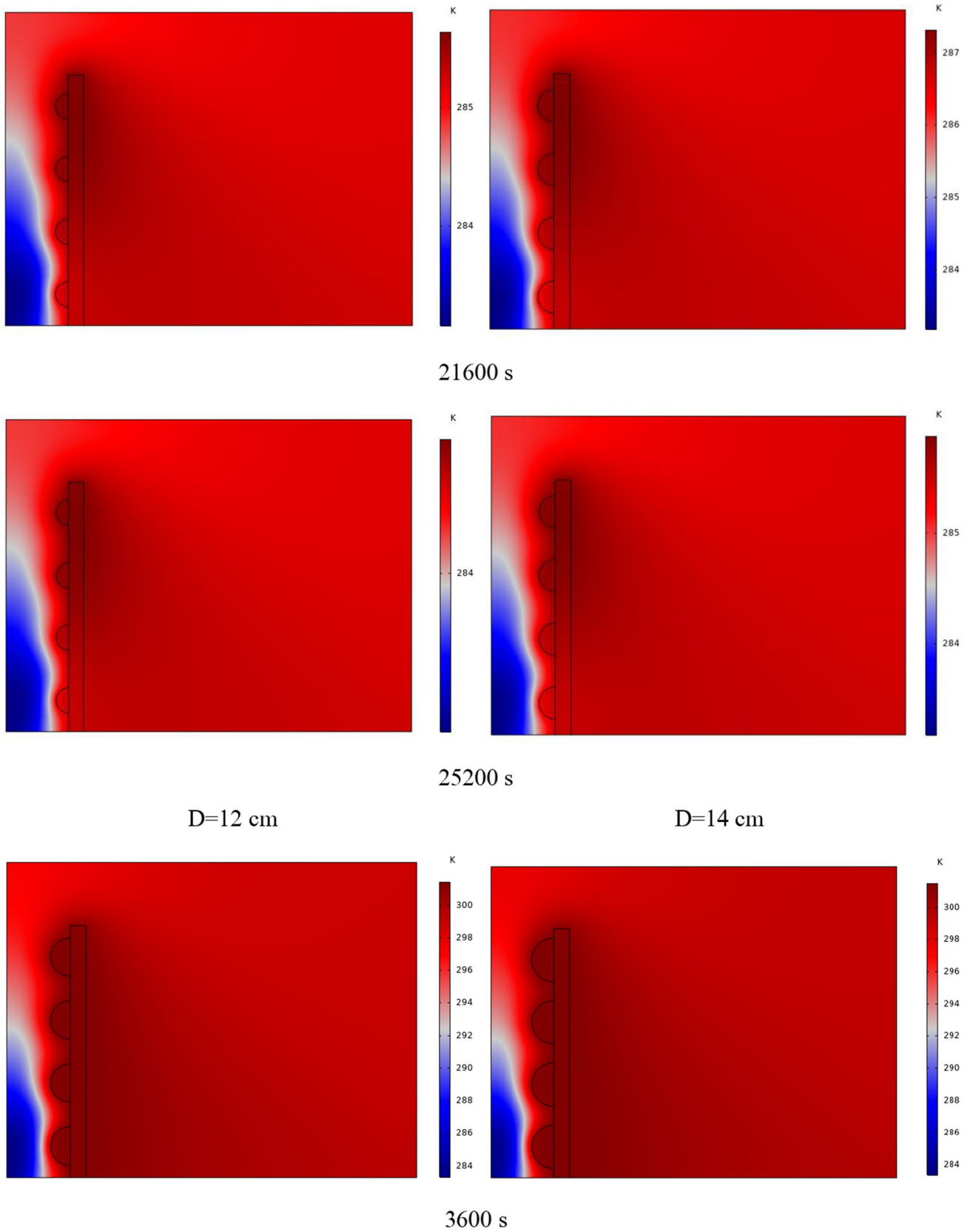


Fig. 4 (continued)

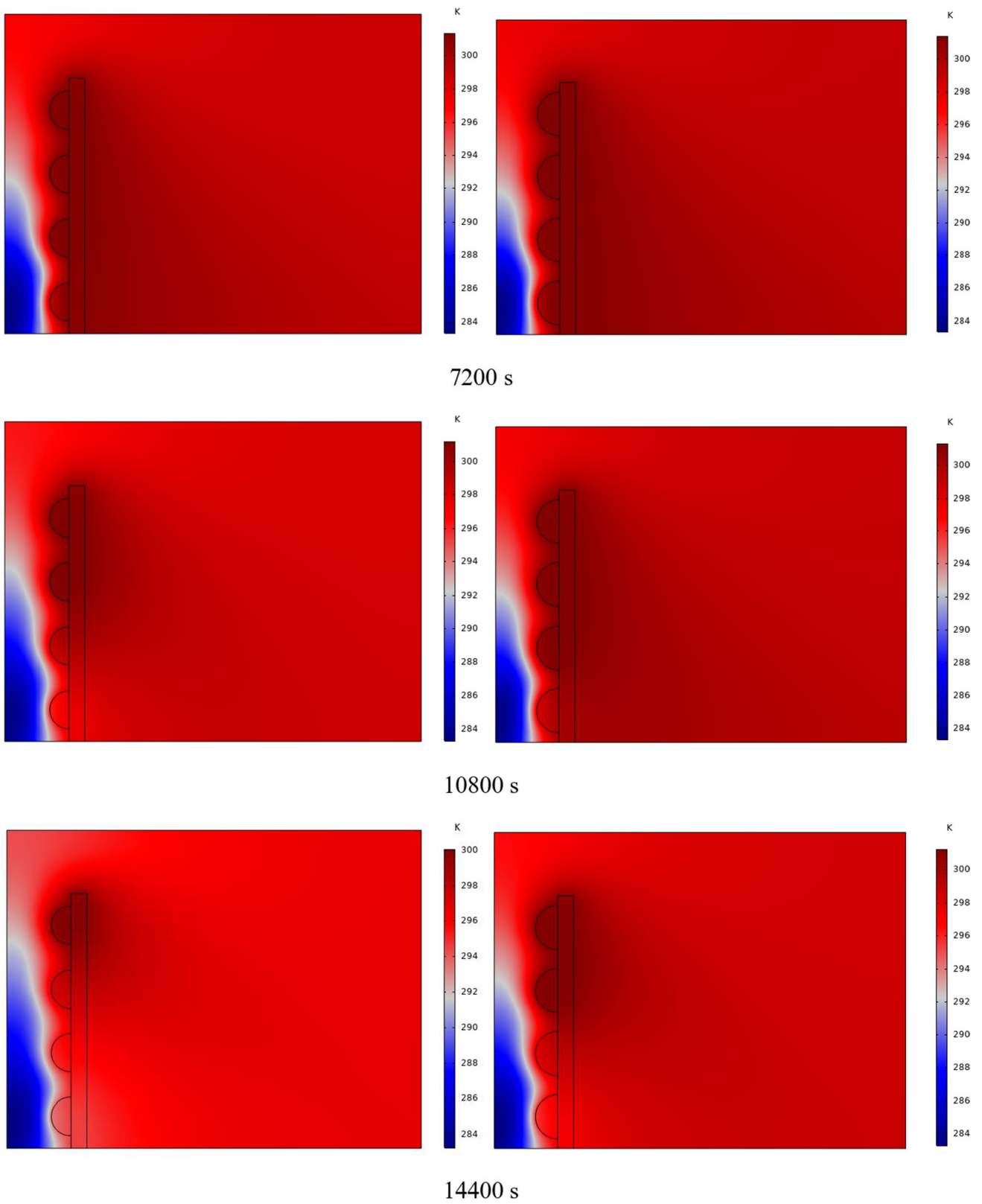


Fig. 4 (continued)

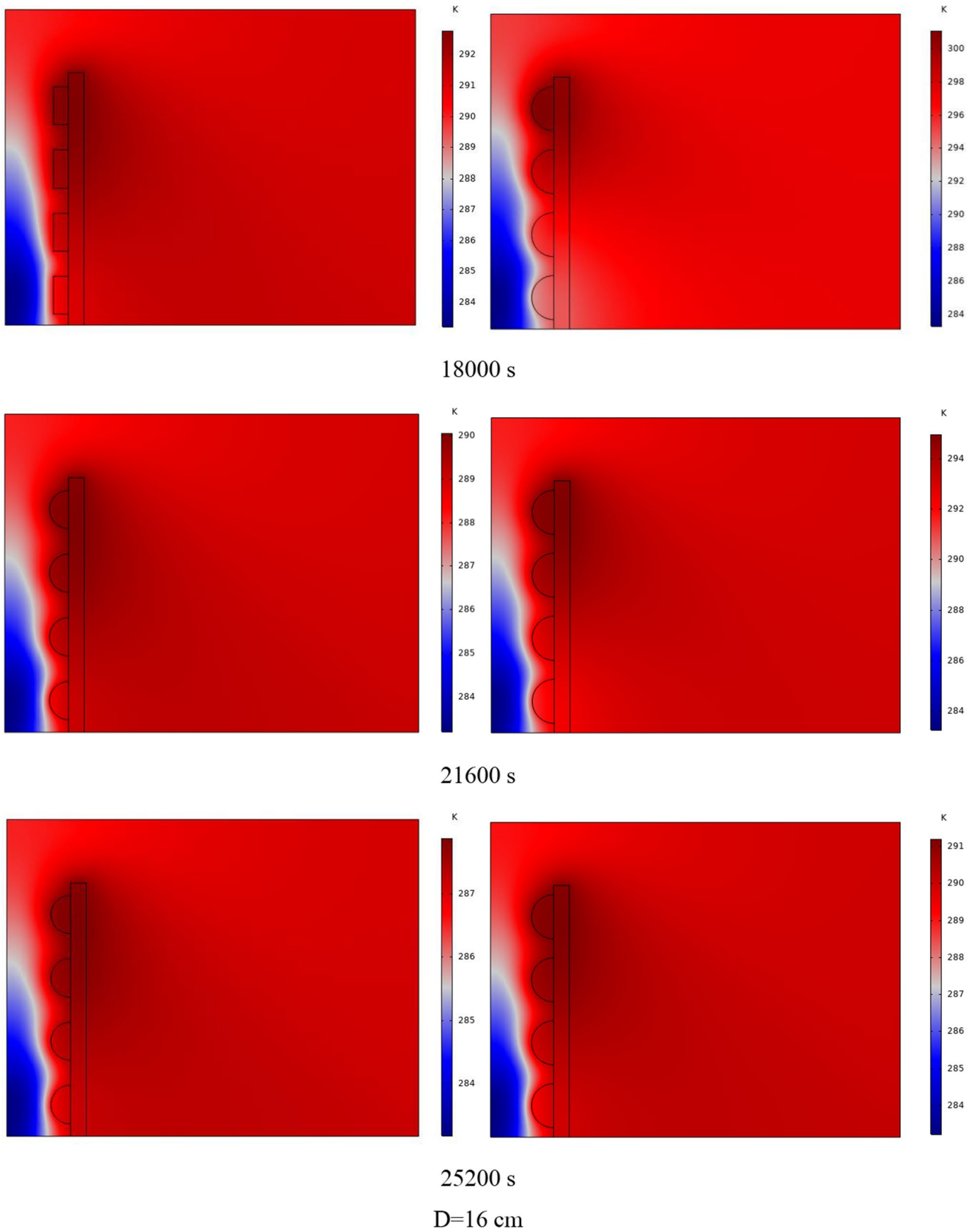


Fig. 4 (continued)

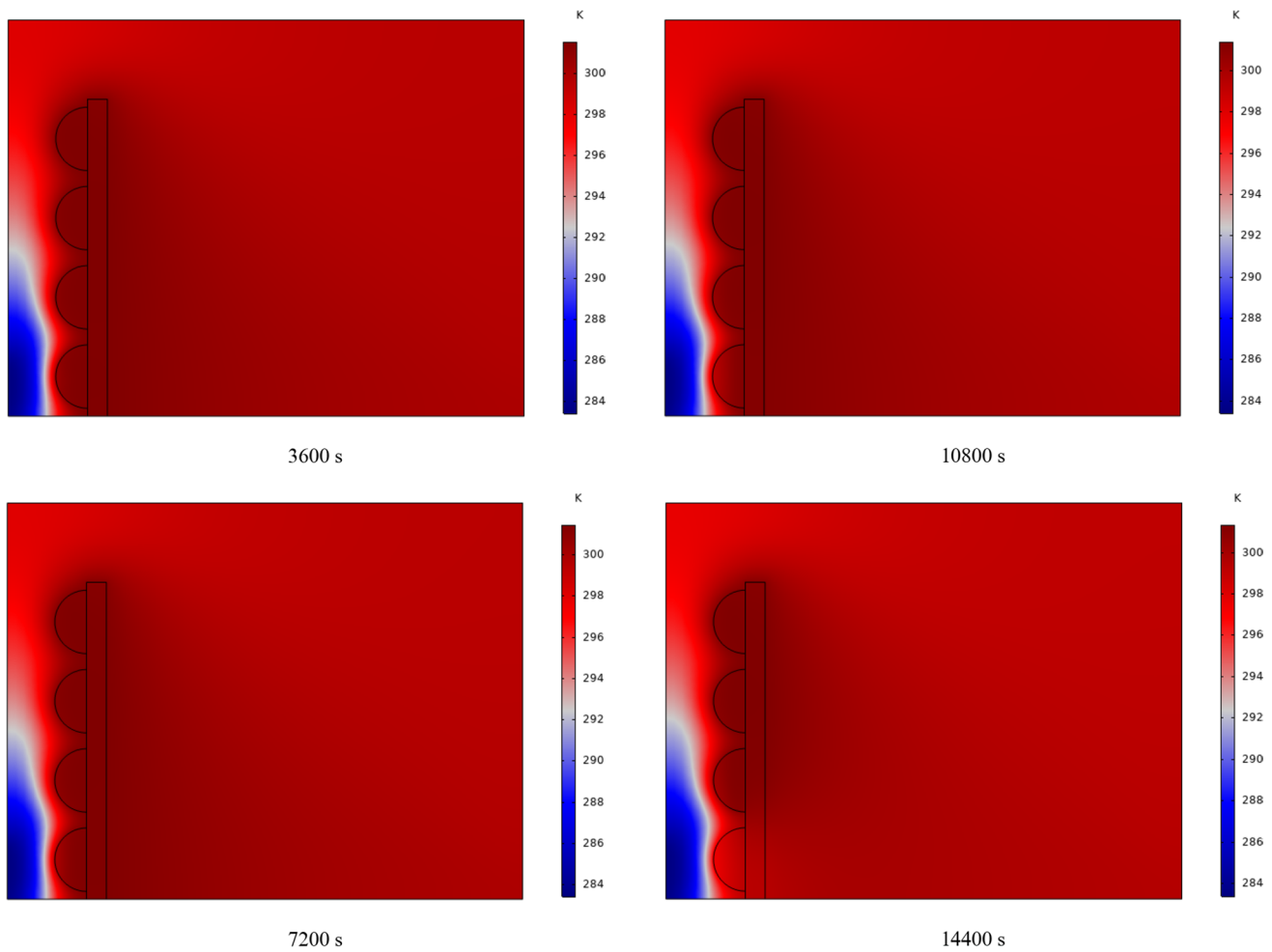


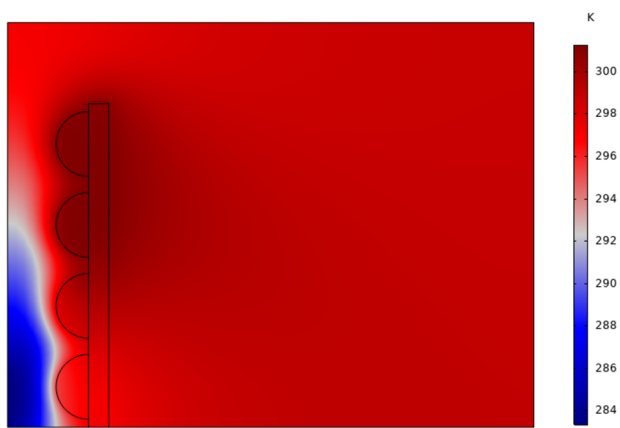
Fig. 4 (continued)

Sergei, Shen et al. 2020). Using solar energy in buildings can ultimately reduce energy consumption (Izadi and El Haj Assad 2021, Jamil, Ali et al. 2021, Usman, Ali et al. 2021).

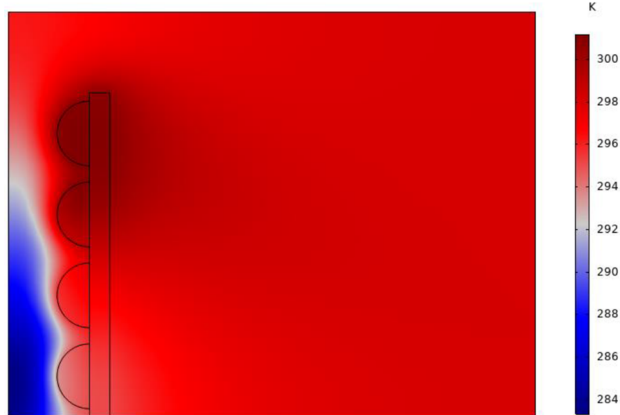
Phase change materials (PCMs) can change phase, for instance, from solid to liquid, in an almost constant temperature range. If PCMs are employed in buildings, storing a large amount of solar energy during the day and using the same energy to heat the space during the night is possible. Therefore, some investigators have examined the use of PCMs in buildings. Lin et al. (2005) employed plates containing stable PCM in underfloor heating systems

Fig. 4 (continued)

with electric heaters to absorb heat during the night when the price of electricity is low and return heat during the day when the price of electricity is high. They used an enclosure containing the reference and test parts. Zhou et al. (2015) evaluated the thermal performance effect of four different geometries of sand and PCM combinations in underfloor heating. It was demonstrated that there are fewer temperature changes by using PCM than by utilizing sand due to the phase change process. The energy release process in using PCM is almost twice as much as using sand in the same experimental conditions. In another study, Aghakhani et al. (2022) revealed the effect of using

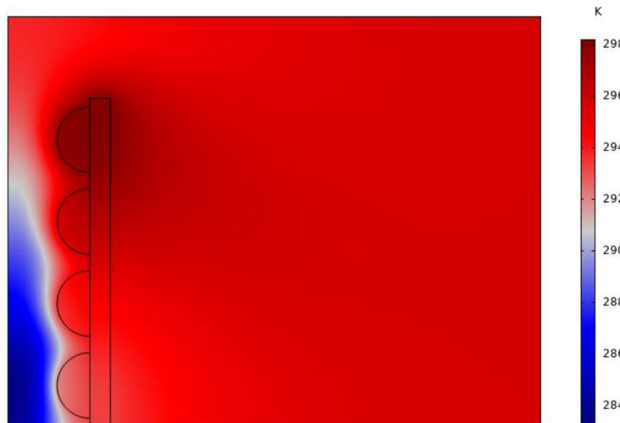


18000 s



21600 s

Fig. 4 (continued)



25200 s

Fig. 4 (continued)

PCM enclosures with different angles in the walls of a building. They assessed the melting contours and volume fraction of molten PCM by changing the dimensions, angle, and number of PCM enclosures. In the meantime, some researchers have employed PCMs in the Trombe wall in buildings so that they can improve their efficiency. In one of these studies, Tlili and Alharbi (2022) numerically examined the impact of PCM in Trombe walls on the freezing/melting processes, by changing the location of PCM blocks in the wall and conducting a transient study. They evaluated the freezing time of PCM and demonstrated that the lower blocks in the wall lost their temperature earlier and solidified faster in the presence of PCM.

Using solar energy and other new and renewable energy in buildings can significantly reduce energy consumption (Kara and Kurnuç 2012, Saadatian, Sopian et al. 2012, Zalewski, Joulin et al. 2012). There are several ways to use solar energy in buildings. One of these methods is to use Trombe walls in buildings. These walls can be used to move air or heat the house (Bojić, Johannes et al. 2014, Bellos, Tzivanidis et al. 2016, Omrany, Ghaffarianhoseini et al. 2016). The short window of time during which solar energy is available is one of the issues and restrictions with utilizing it. Utilizing PCM in the wall is one strategy for storing solar energy (Jamil, Ali et al. 2021, Lawag and Ali 2022). PCMs have the capacity to store thermal energy in their bodies, such as solar thermal energy. (Elghamry and Hassan 2020, Khetib, Alotaibi et al. 2021, Oluah, Akinlabi et al. 2021). With this in mind, this paper simulates a Trombe wall with PCM. On the wall, there are a number of obstacles with two shapes of semicircle and rectangle full of PCM. The varying dimensions of obstructions were studied without the benefit of sun hours. Additionally, the impact of two different types of impediments working together on the wall's efficiency time has been studied.

### Problem definition

The wall being analyzed is set up in a space that measures 2 by 3 m and has a ceiling height of 2.8 m. The whole wall is made of concrete, and four cavities with organic PCM have been placed. The two barrier shapes under consideration include a semicircle and a rectangle as shown in Fig. 1. Parameter D (aspect ratio) has been changed from 8 to 16 cm for two obstacles. This

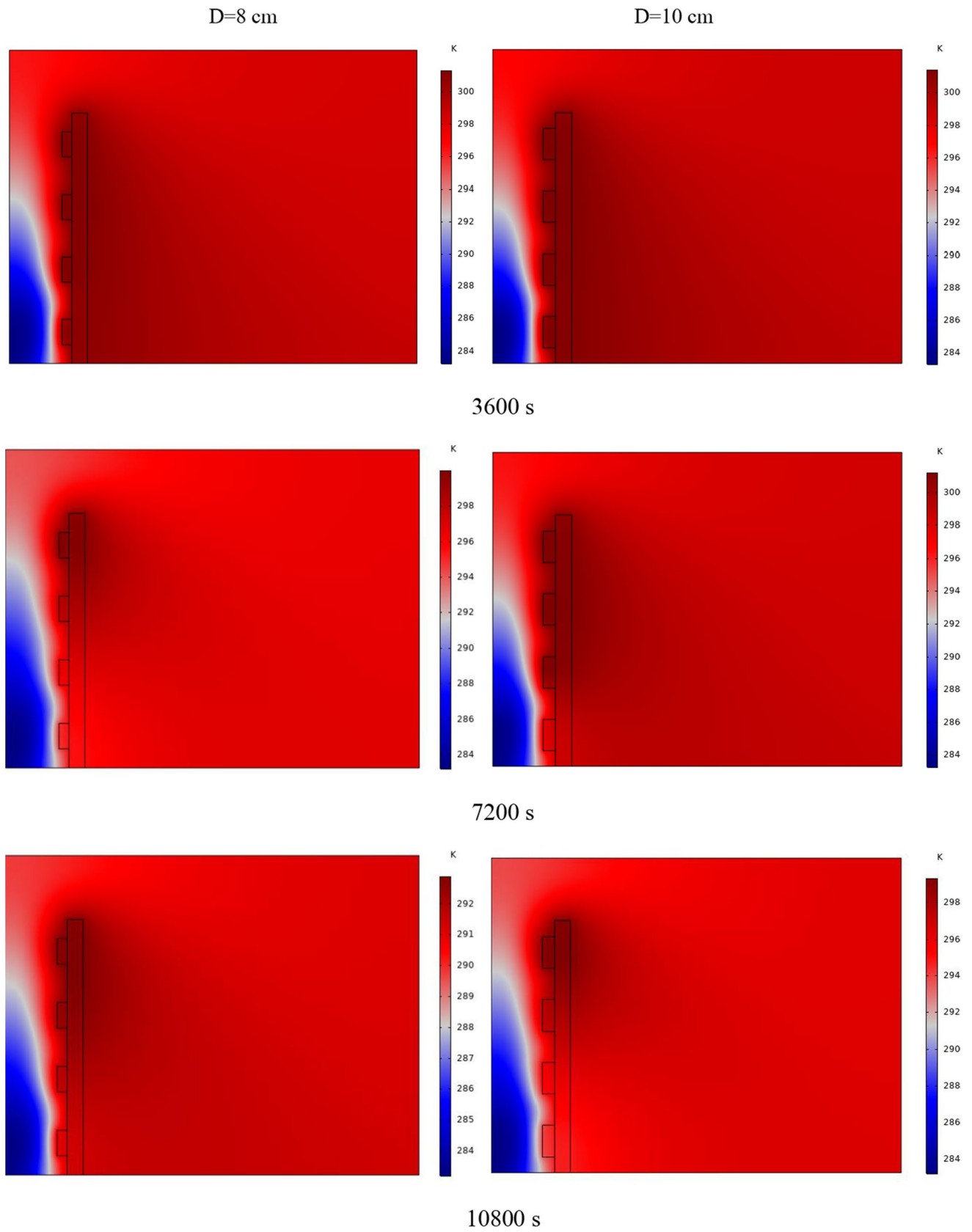


Fig. 5 Temperature contour on the wall from 1 to 7 h for (D) 8 to 16 cm for RECs

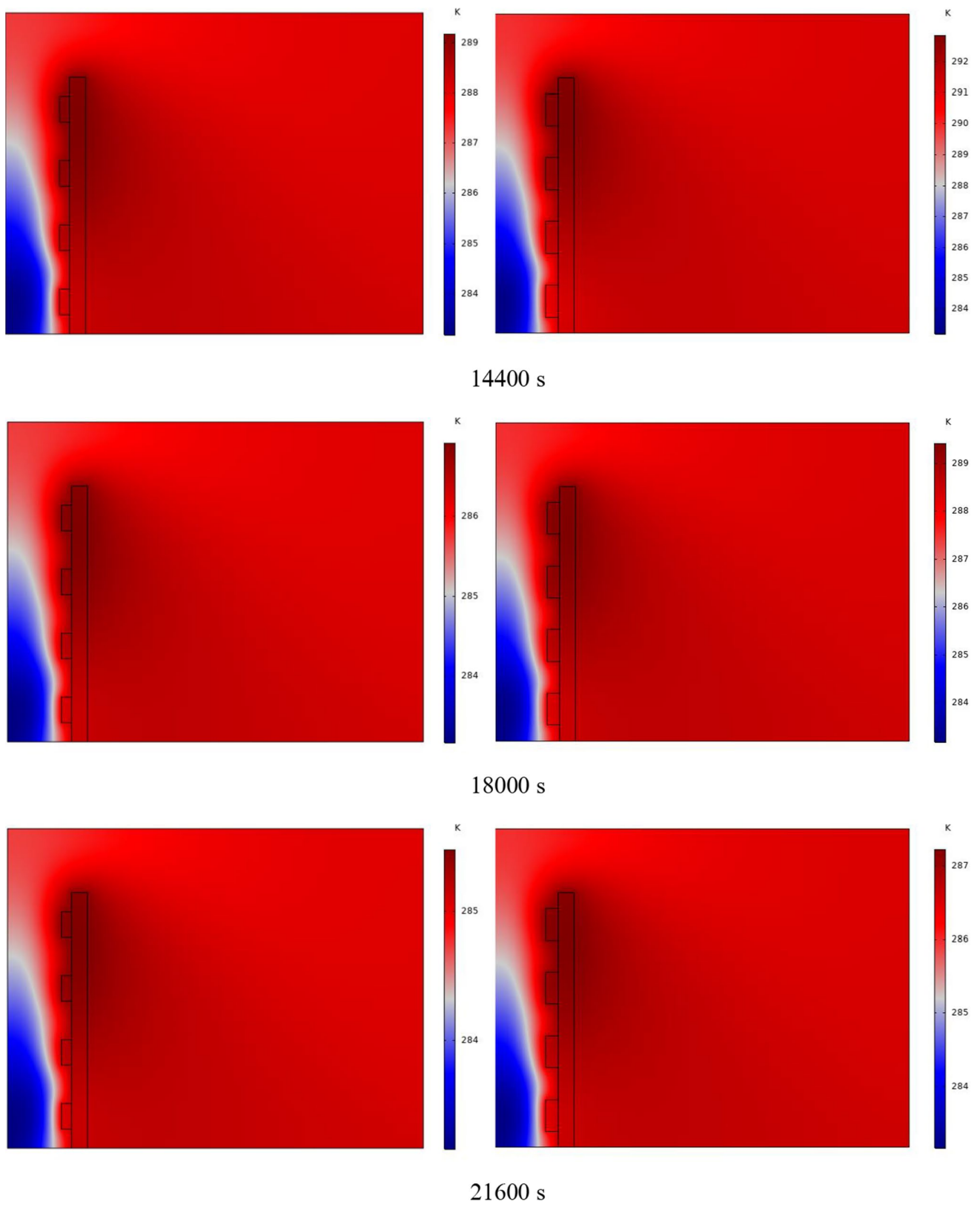


Fig. 5 (continued)

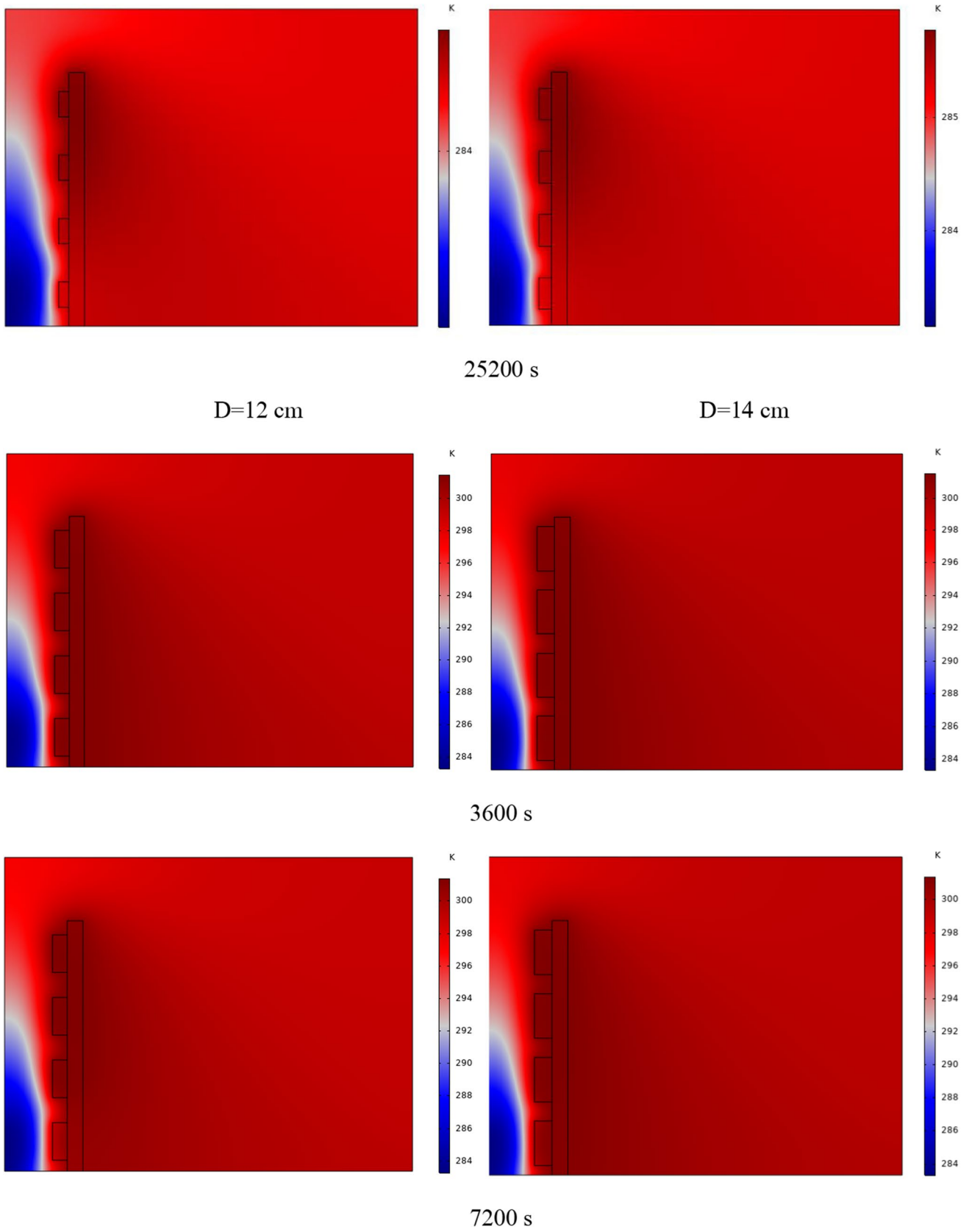


Fig. 5 (continued)

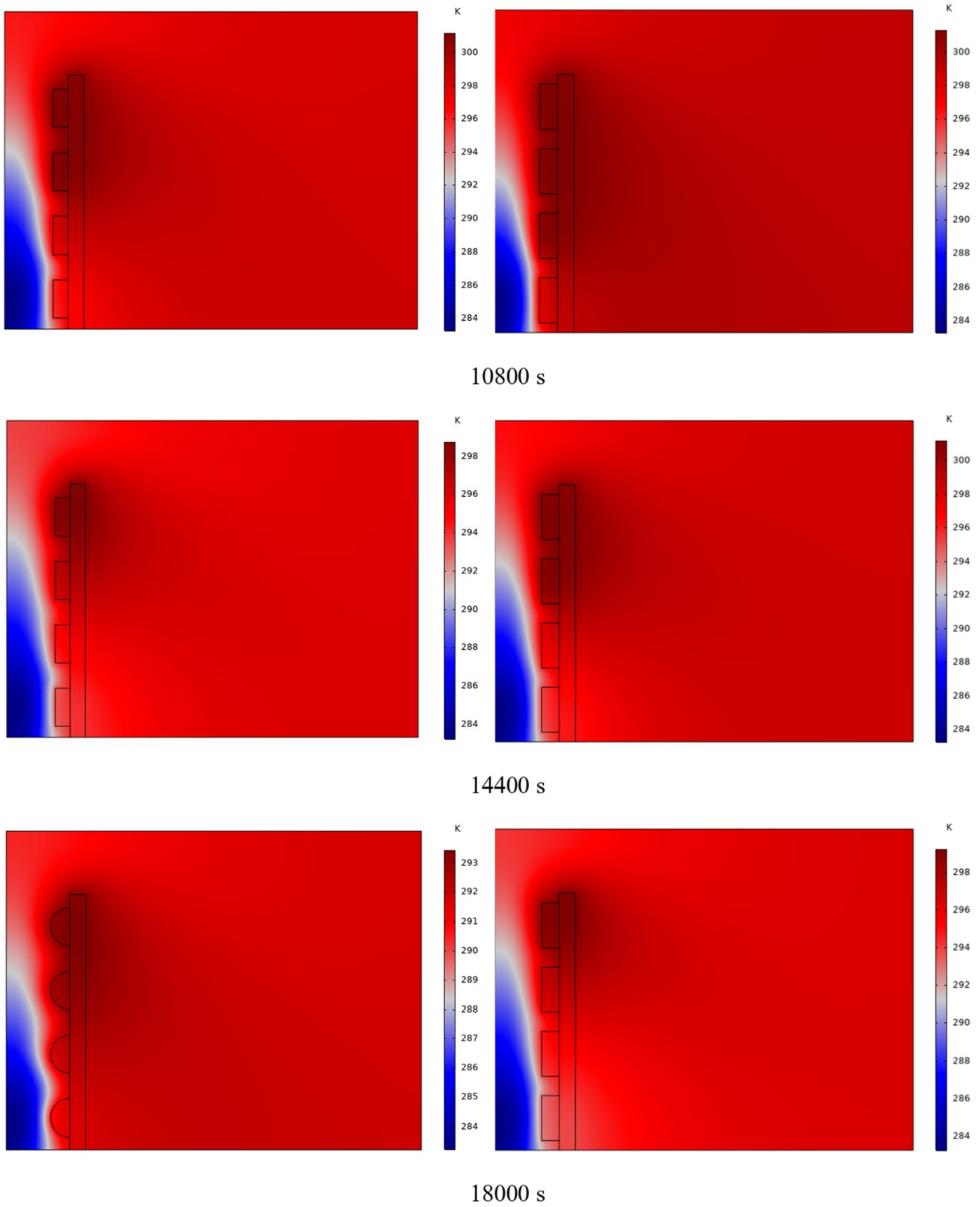
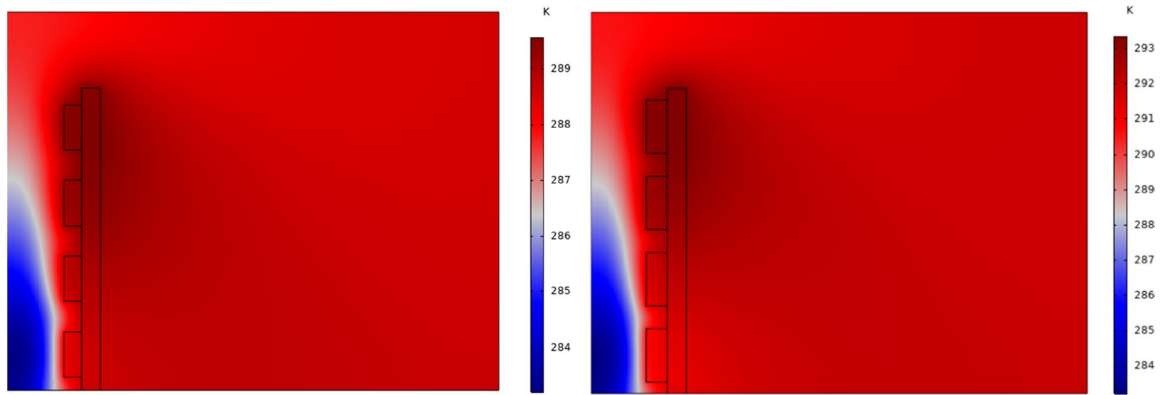
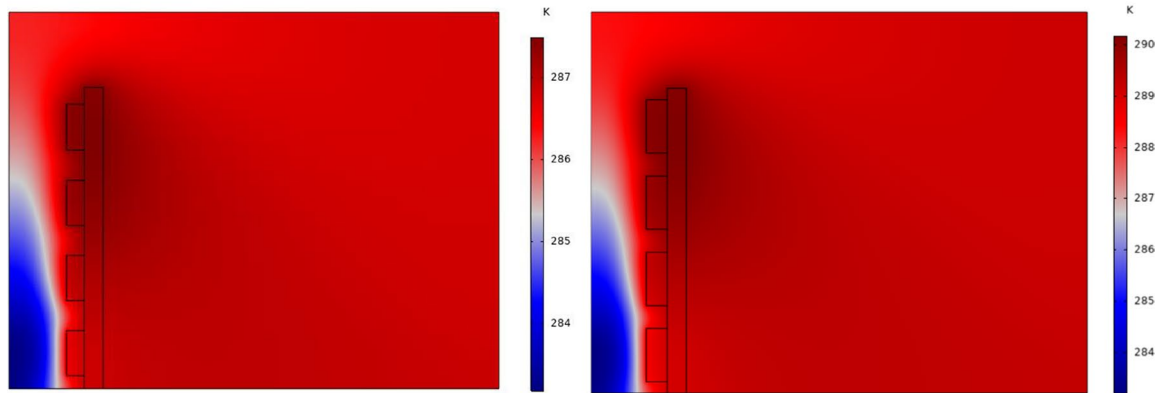


Fig. 5 (continued)

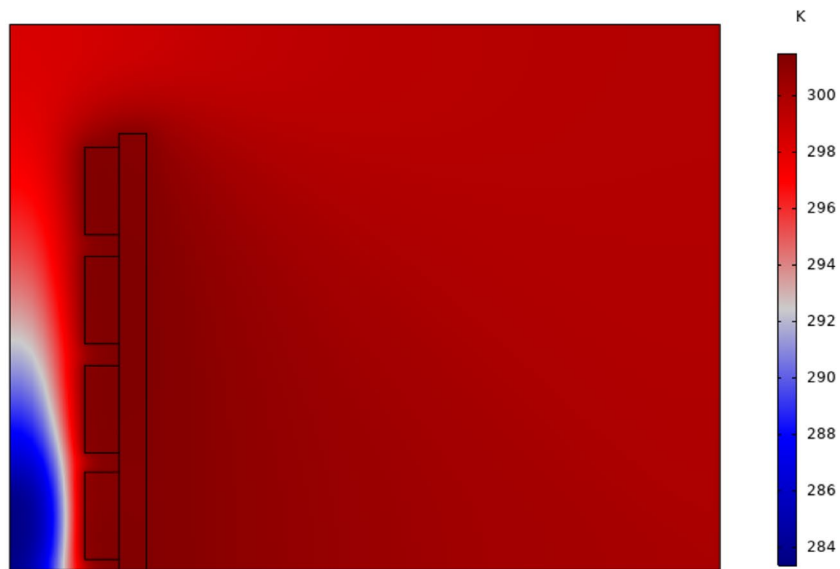


21600 s



25200 s

D=16 cm



3600 s

Fig. 5 (continued)

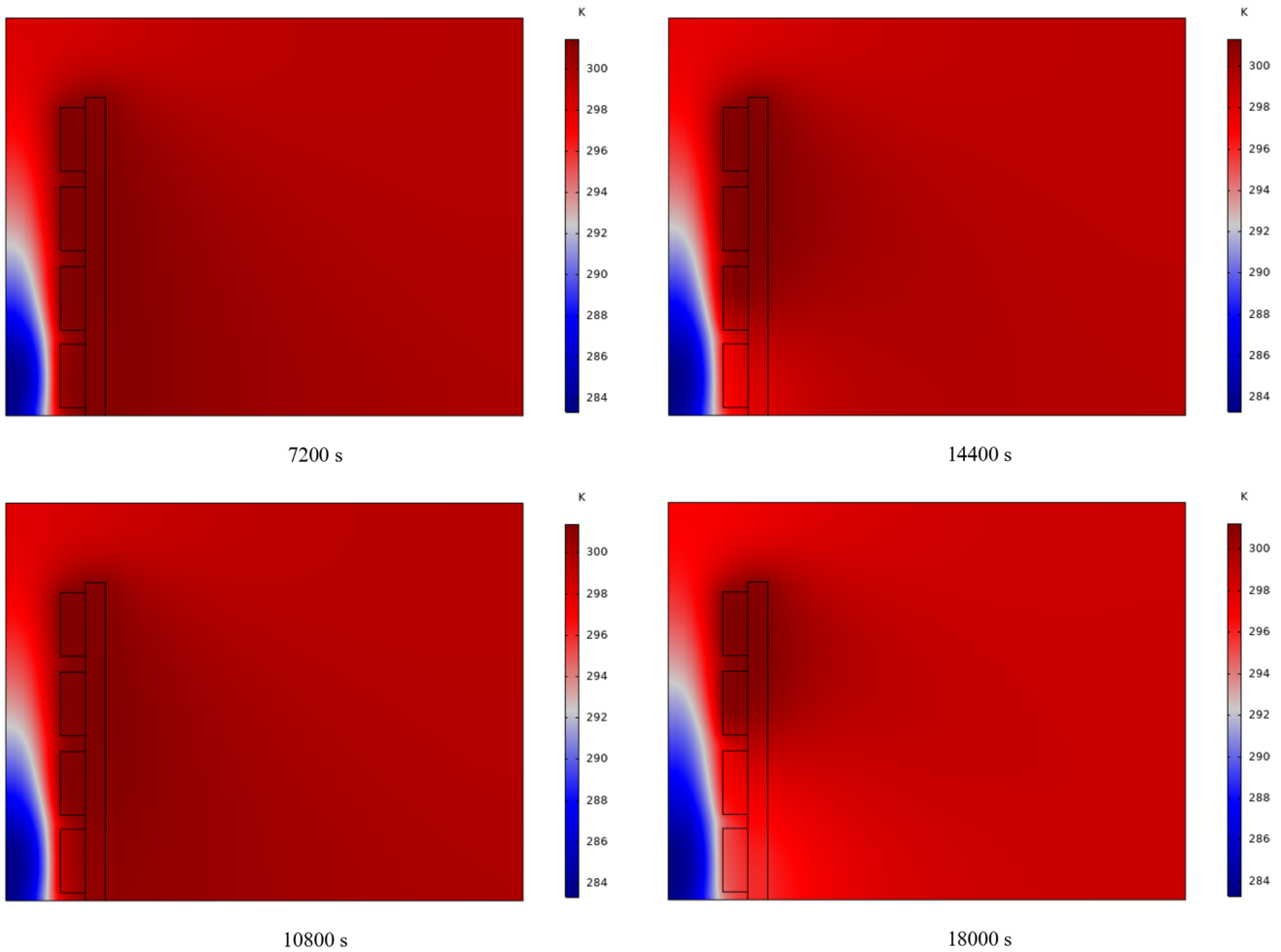


Fig. 5 (continued)

parameter represents the radius of the semicircle for the SEC and the width of the rectangle for the REC. This analysis was done for the duration of the night, so the amount of solar radiation was equal to 0, and the temperature of the wall was equal to the temperature of the PCM in the molten state. Also, the inlet air temperature is 10 °C, and the wind speed is considered to be a constant value of 1 m/s. It is noteworthy that the length of the rectangle is chosen in each step so that the volume of PCM used in both REC and SECs is equal. The PCM (gallium) is utilized in the walls (Yang, Tan et al. 2016). Table 1 shows the thermo-physical properties of gallium.

Because of the free convection of air at home, buoyancy is also a factor in the equation. For this problem, the Boussinesq approximation has been utilized. The ensuing equations are shown as follows.

Fig. 5 (continued)

$$\frac{\partial u}{\partial x} + \frac{\partial v}{\partial y} = 0 \tag{1}$$

$$\frac{\partial u}{\partial t} + u \frac{\partial u}{\partial x} + v \frac{\partial u}{\partial y} = -\frac{1}{\rho} \frac{\partial p}{\partial x} + \frac{1}{\rho} \left( \frac{\partial}{\partial x} \left( \mu \frac{\partial u}{\partial x} \right) + \frac{\partial}{\partial y} \left( \mu \frac{\partial u}{\partial y} \right) \right) \tag{2}$$

$$\frac{\partial v}{\partial t} + u \frac{\partial v}{\partial x} + v \frac{\partial v}{\partial y} = -\frac{1}{\rho} \frac{\partial p}{\partial y} + \frac{1}{\rho} \left( \frac{\partial}{\partial x} \left( \mu \frac{\partial v}{\partial x} \right) + \frac{\partial}{\partial y} \left( \mu \frac{\partial v}{\partial y} \right) \right) + g\beta(T - T_c) \tag{3}$$

$$\frac{\partial T}{\partial t} + \left( u \frac{\partial T}{\partial x} + v \frac{\partial T}{\partial y} \right) = \frac{k_{nf}}{\rho C_p} \left( \frac{\partial^2 T}{\partial x^2} + \frac{\partial^2 T}{\partial y^2} \right) \tag{4}$$

To solve the PCM solidification and melting issues, it is necessary to solve the equations of mass, momentum, and energy survival in it. The following equations are given for PCM.

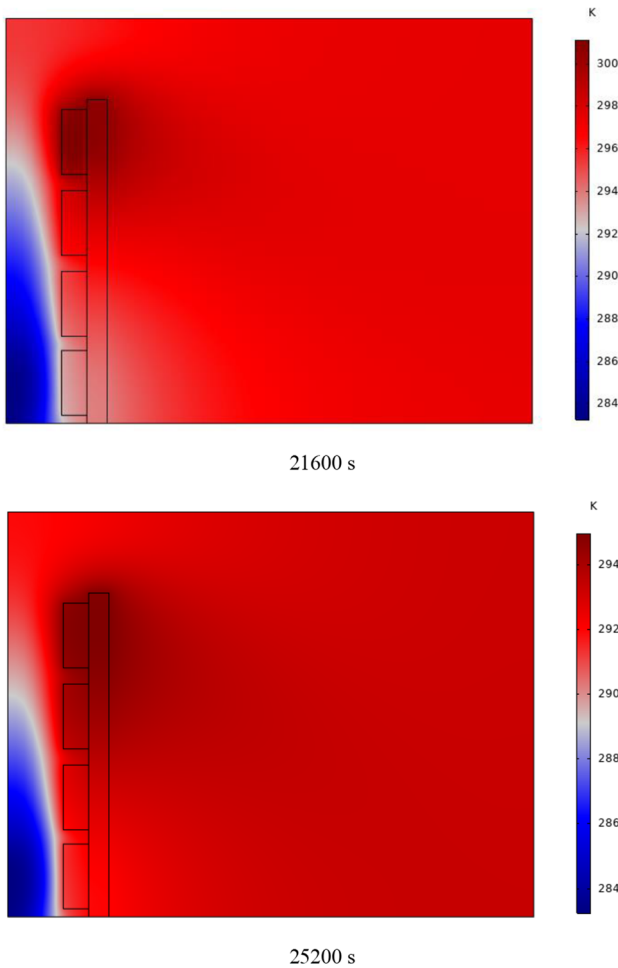


Fig. 5 (continued)

$$\frac{\partial \rho}{\partial t} + \nabla \cdot (\rho \vec{v}) = 0 \tag{5}$$

$$\frac{\partial}{\partial t} (\rho \vec{v}) + \nabla \cdot (\rho \vec{v} \vec{v}) = -\nabla p + \rho \vec{g} + \nabla \cdot \vec{\tau} + \vec{F} \tag{6}$$

$$\frac{\partial(\rho h)}{\partial t} + \nabla \cdot (\rho \vec{v} H) = \nabla \cdot (k \nabla h) + S \tag{7}$$

In the momentum equation, term F is defined as  $A_m \frac{(1-\beta)^2}{\beta^3 + 0.001}$  according to the references.  $A_m$  value is  $10^5$ . The difference between the melting's start and finish points leads to the establishment of a parameter known as beta ( $\beta$ ).  $\beta$  is the paraffin liquefaction fraction, which is 0 before melting begins and one after the paraffin is

entirely liquefied and is a value between zero and one in the melting range.  $B$  is the Boltzmann coefficient with a value of  $1.38 \times 10^{-23} J/K$ . The (Arasu and Mujumdar 2012) following equations are given for obtaining  $\beta$ .

$$\beta_k = \begin{cases} \beta = 0 & \text{if } T < T_{solidus} \\ \beta = 1 & \text{if } T > T_{Liquidus} \\ \beta = \frac{T - T_{solidus}}{T_{Liquidus} - T_{solidus}} & \text{if } T_{Liquidus} \leq T \leq T_{solidus} \end{cases} \tag{8}$$

### Numerical method and grid study

COMSOL software was utilized to create the wall simulation. The equations were also algebraized using the finite element approach. A variety of distinct components is investigated in the grid created on the geometry. Finally, the primary mesh for the SEC was chosen at 428 thousand elements, and the number of meshes for the REC was chosen at 465 thousand elements. Figure 2 shows the impact of the number of grid elements on the TAR escaping the wall and the wall's temperature for the two SEC and RECs.

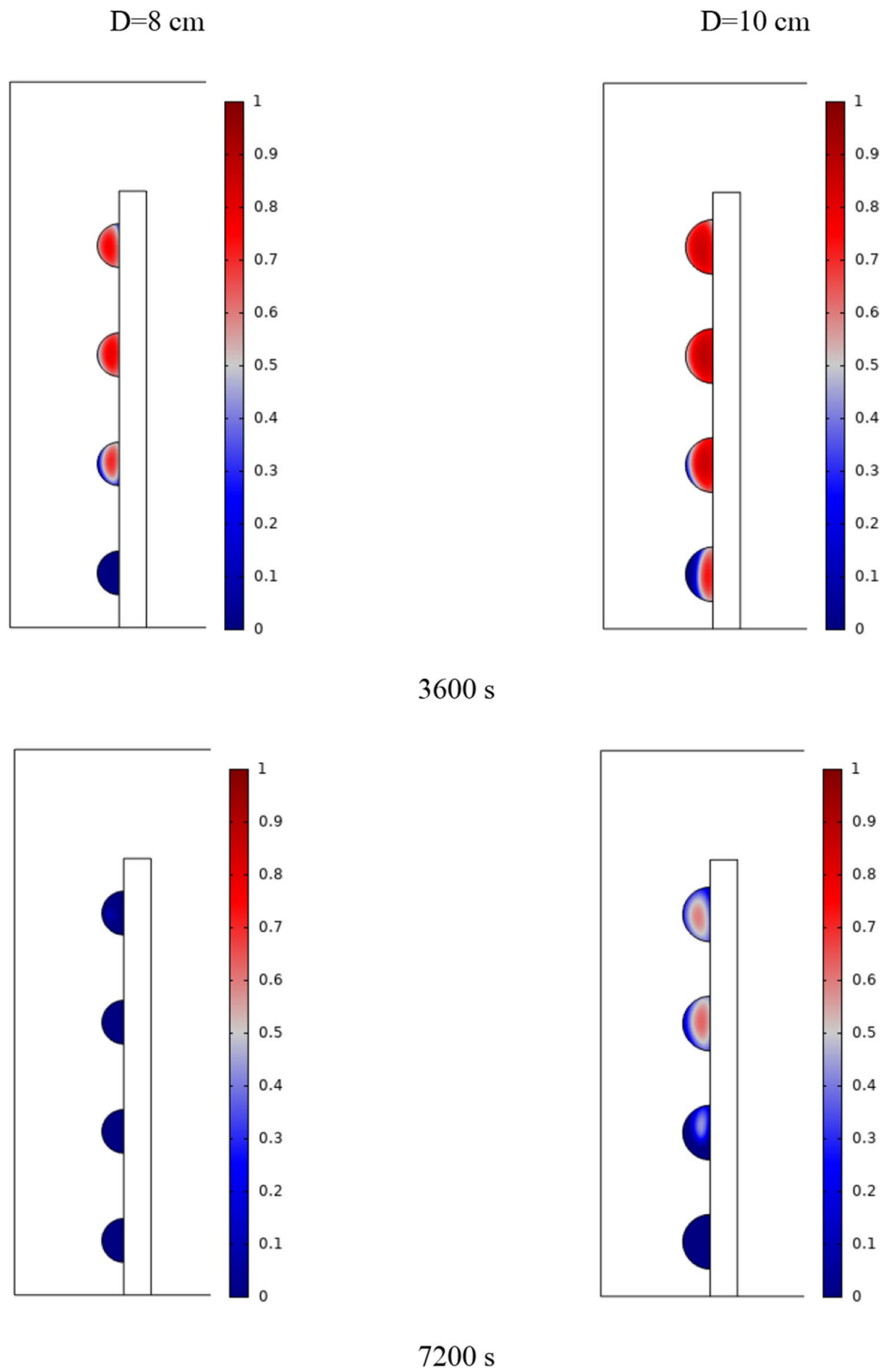
### Validation

To verify the results, a validation using the paper Bouhal et al. (2018) has taken place. In this validation, which is given in Fig. 3, the amount of molten PCM at different times between the present work and the article (Bouhal, ed-Dîn Fertahi et al. 2018) is given. The findings of this simulation are acceptable given the error of less than 5% between this study and the validation data.

### Results and discussion

In Fig. 4, the temperature contour on the wall is enclosed for 1 to 7 h for (D) 8 to 16 cm for SECs. According to the wall, it can be seen that the amount of TWL is largely dependent on the obstacles. In the absence of solar radiation, the wall, which has a low heat capacity, loses its temperature in a short time. These cavities, despite the PCM, maintain the TWL due to the latent heat inside. So, the parts of the wall where the PCM solidifies faster

**Fig. 6** PCM freezing contour inside cavities, from different times, for D 8 to 16 cm for SECs

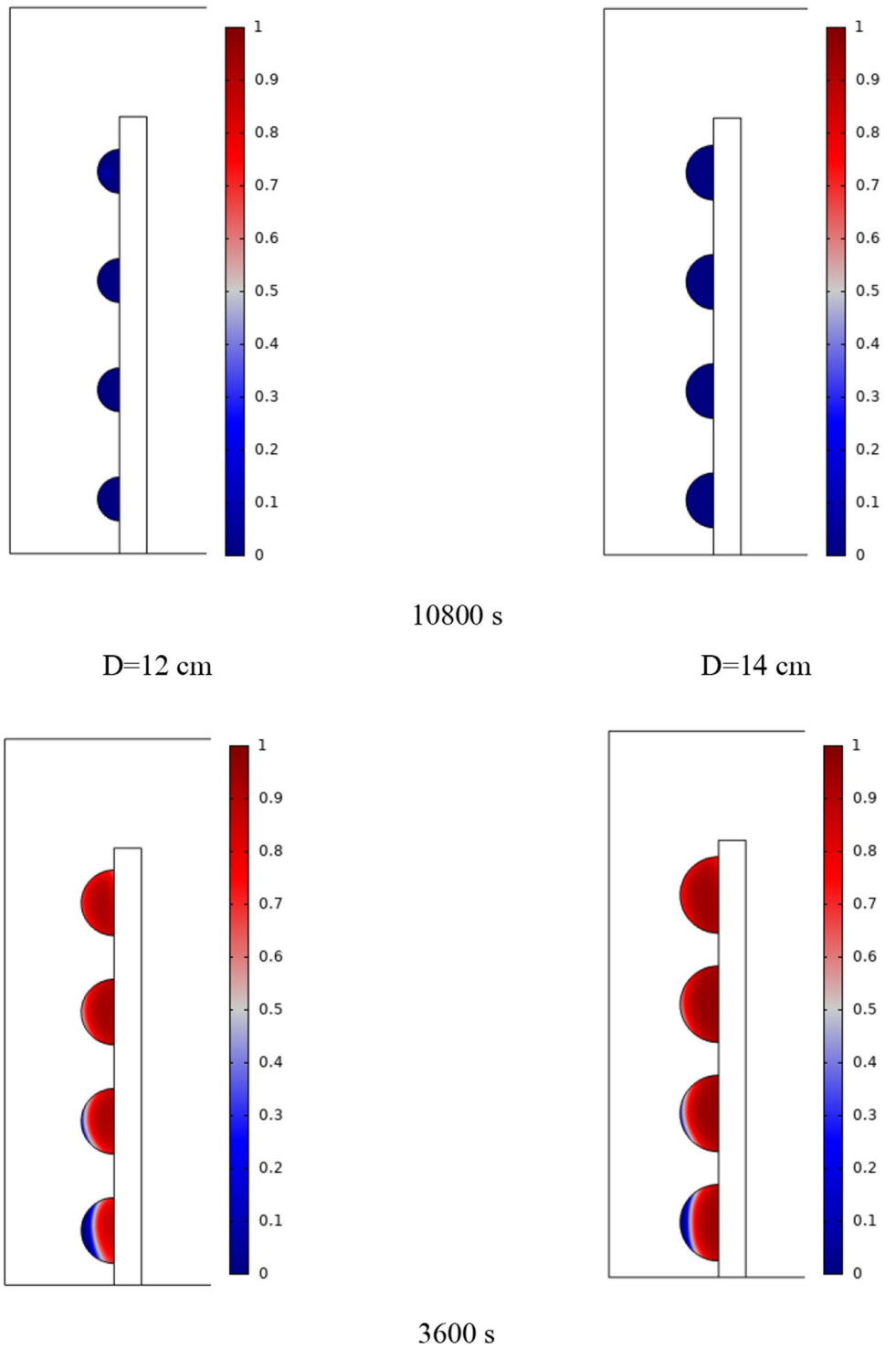


in front of the cavities lose their temperature sooner. The hottest part of the wall is the top, where the molten PCM remains most of the time. The larger the barrier, the more PCM is used in front of the wall, so the molten PCM stays in front of the barrier for longer. So, for more time, the

TWL has been in high value. At an aspect ratio of 8 cm, the TWL decreased slightly in time, and even at 7 h, the TWL approached the inlet TAR.

The temperature contour on the wall is from 1 to 7 h for (D) 8 to 16 cm for RECs, as illustrated in Fig. 5. Cold air

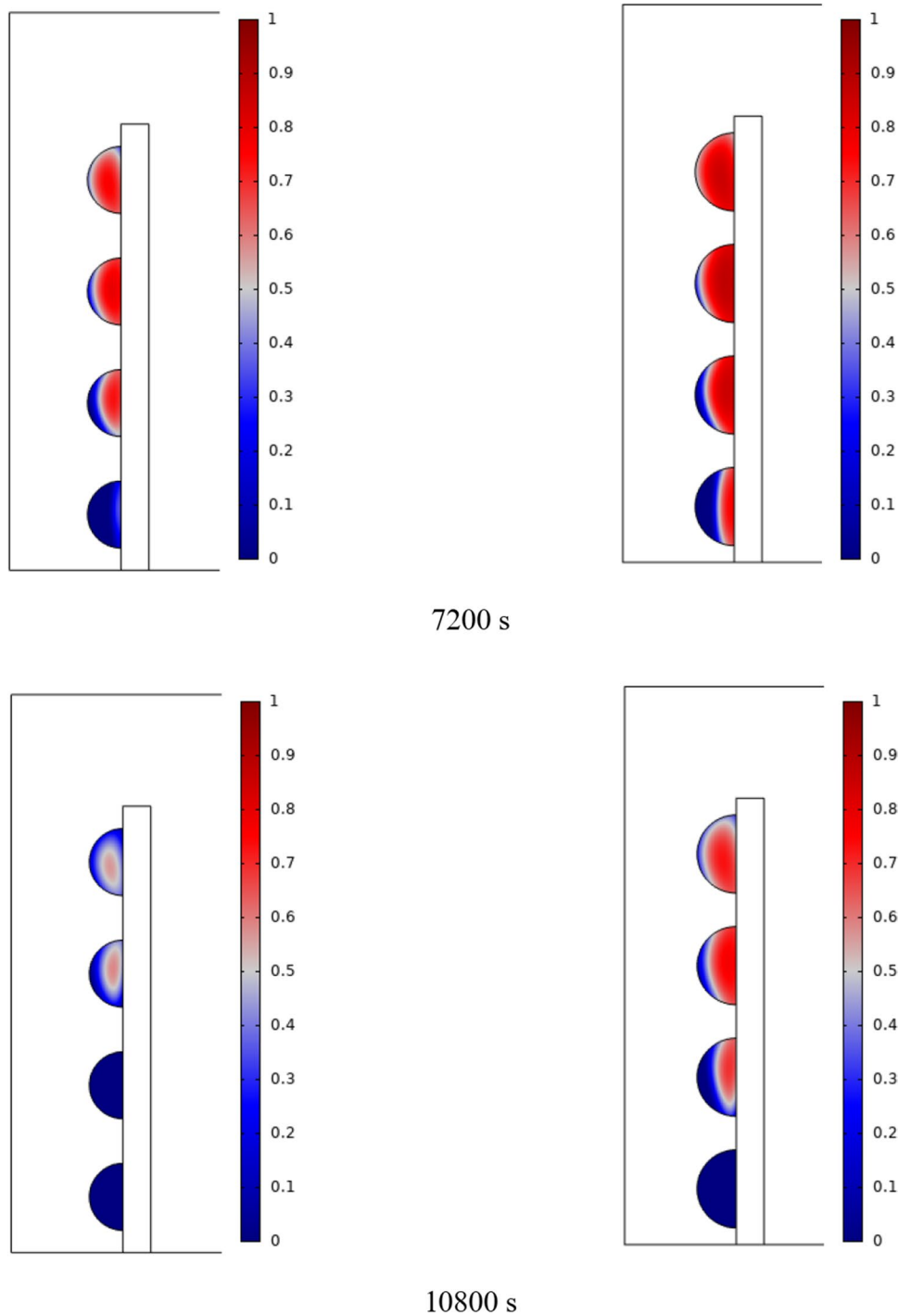
Fig. 6 (continued)



has experienced an increase in temperature after entering and hitting the wall and moving upwards. The latent energy inside the PCM is transferred to the air, and as a result, the air is heated, and the air that is warmer than the inlet is

directed into the room. At the beginning of the process, due to the warmer wall and also more molten PCM in the obstacles, the TAR leaving the wall was higher. The temperature of the air leaving the wall falls with time and eventually

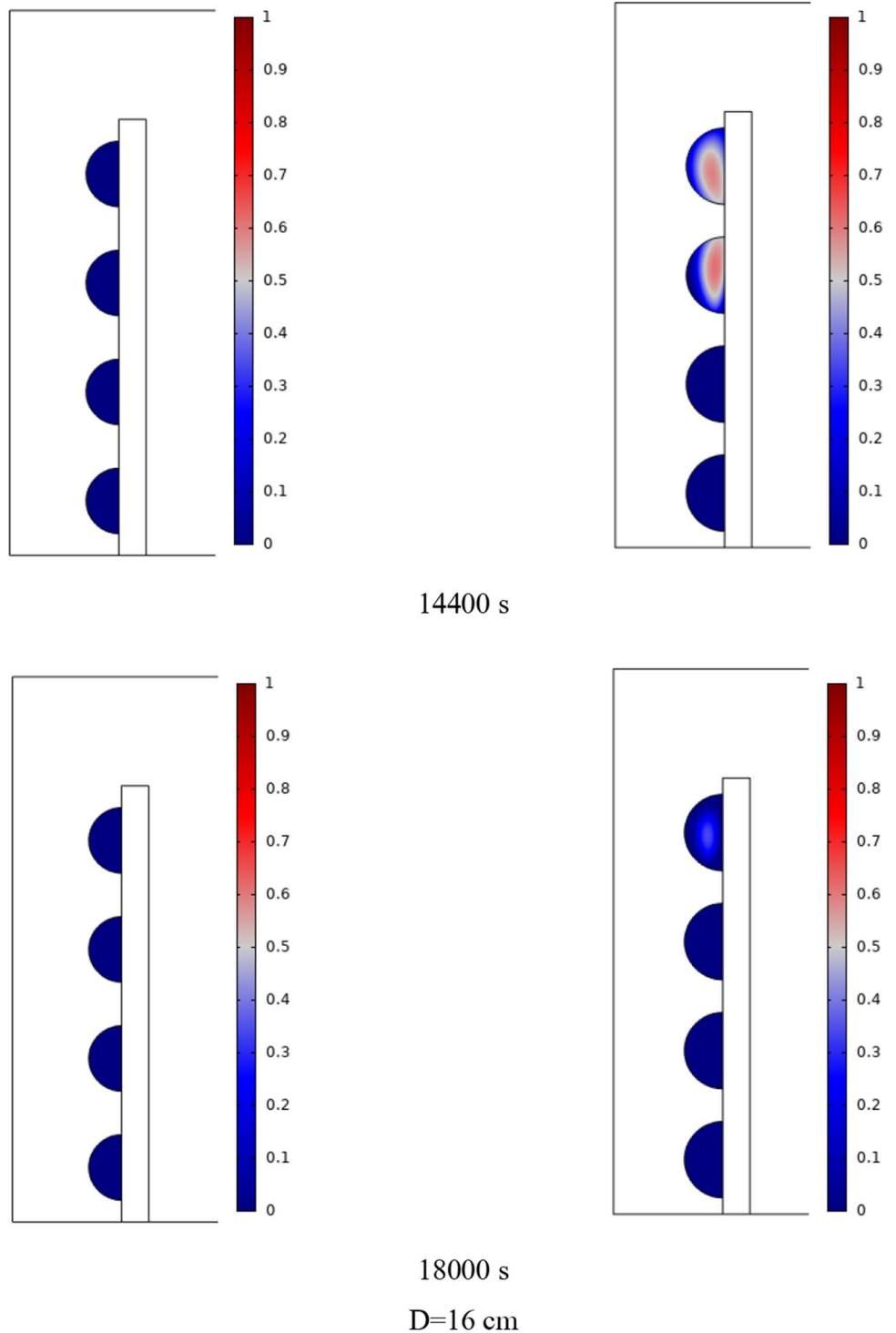
Fig. 6 (continued)



approaches the temperature of the air entering the wall. The outlet air's temperature is lower than the wall's due to a decrease in the temperature of the wall and a reduction in the molten PCM in the cavities. As all PCM values solidify within the cavities, the TAR decreases sharply and closer to the inlet temperature.

The PCM freezing contour within the cavities is shown in Fig. 6 for (D) 8 to 16 cm for SECs at various periods. A value of zero in the legend indicates a completely solid PCM, and a value of 1 indicates an entirely molten PCM. In SECs, the parts inside the SEC arc first lose their heat, and frozen PCM is seen. The lower barrier is initially frozen by

Fig. 6 (continued)

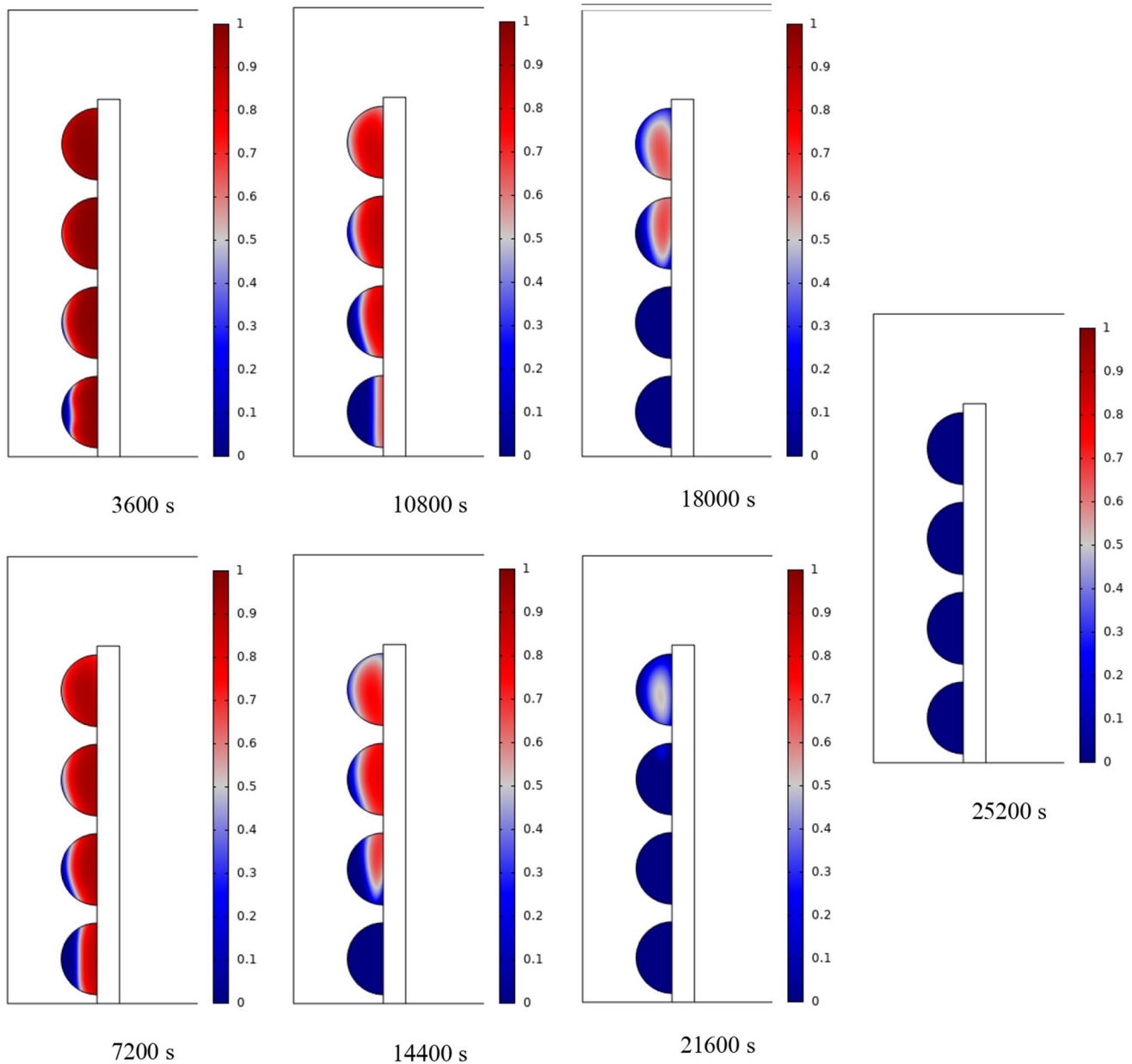


air, and the upper barrier is solidified at the end. The larger the barrier, the more PCM there is in the barrier, and the longer it takes to solidify. The time required for all PCMs to solidify at an aspect ratio of 16 cm is much longer than the aspect ratio of 8 cm. In such a way that for an aspect ratio

of 8 and 10 cm, less than 2 and 3 h were required for the complete freezing of PCM. The above two obstacles become completely solid in the last possible times.

Figure 7 shows the PCM freezing contour inside the cavities, from different times, for (D) 8 to 16 cm for RECs.

Fig. 6 (continued)

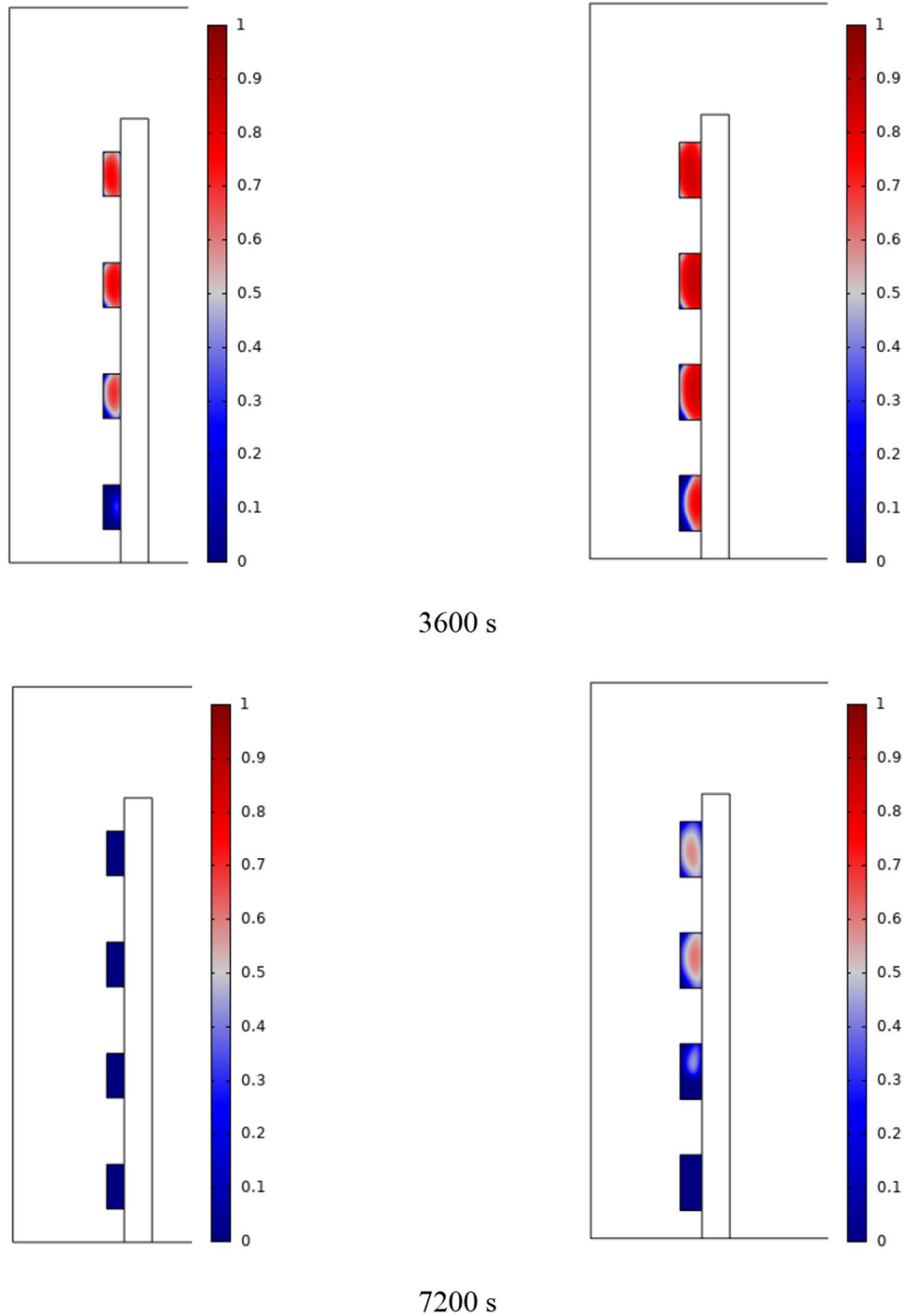


PCM solidification begins at the sharp corners of RECs and then gradually expands inward. The sharp corners of the cavities have more contact with the air, and as a result, they lose their heat faster and become a frozen PCM. The shortest time for PCM to freeze occurred at an aspect ratio of 8 cm, while the longest time for PCM to freeze occurred at an aspect ratio of 16 cm. Comparing the two shapes

of RECs and SECs, it can be seen that the freezing time of PCM in RECs is a little less, and the freezing process shows a little faster in its RECs. Especially in the 16 cm aspect ratio in the freezing process, it was faster in REC than in SEC.

The output TAR from the front of the Trombe wall at various (D)s, from 8 to 16 cm, from 0 to 7 h, is shown

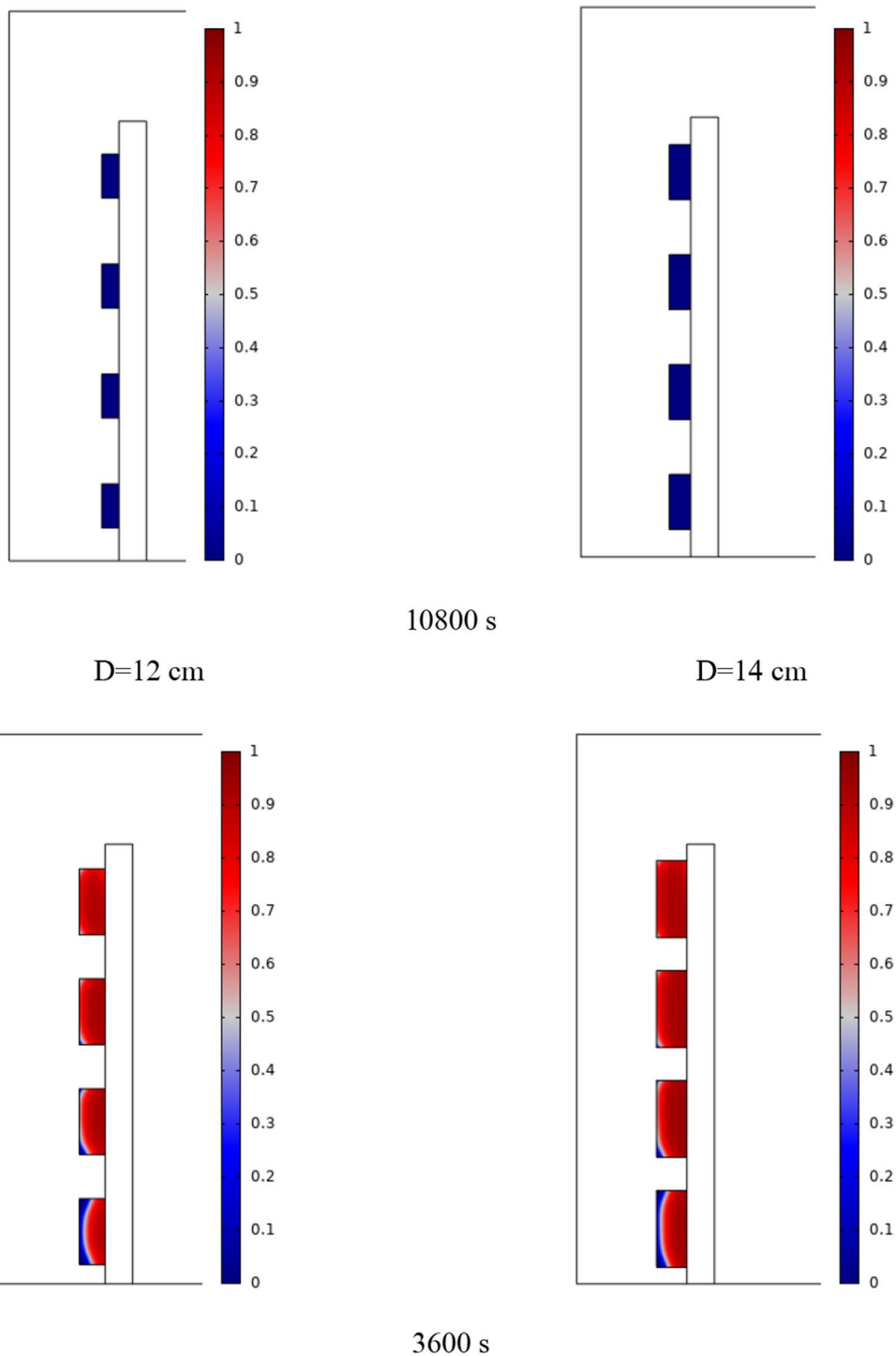
**Fig. 7** PCM freezing contour inside cavities, from different times, for (D) 8 to 16 cm for RECs



in Fig. 8 for SECs. The TAR departing the wall is higher than the temperature entering the wall because of solar radiation. The energy stored in the wall and the PCM is trapped behind the cavities during the night when solar

radiation fails to raise the TAR in front of the wall. As a result, the temperature of the exit air is higher than the temperature of the input air. The wall can only temporarily boost the TAR in front of it because of its limited

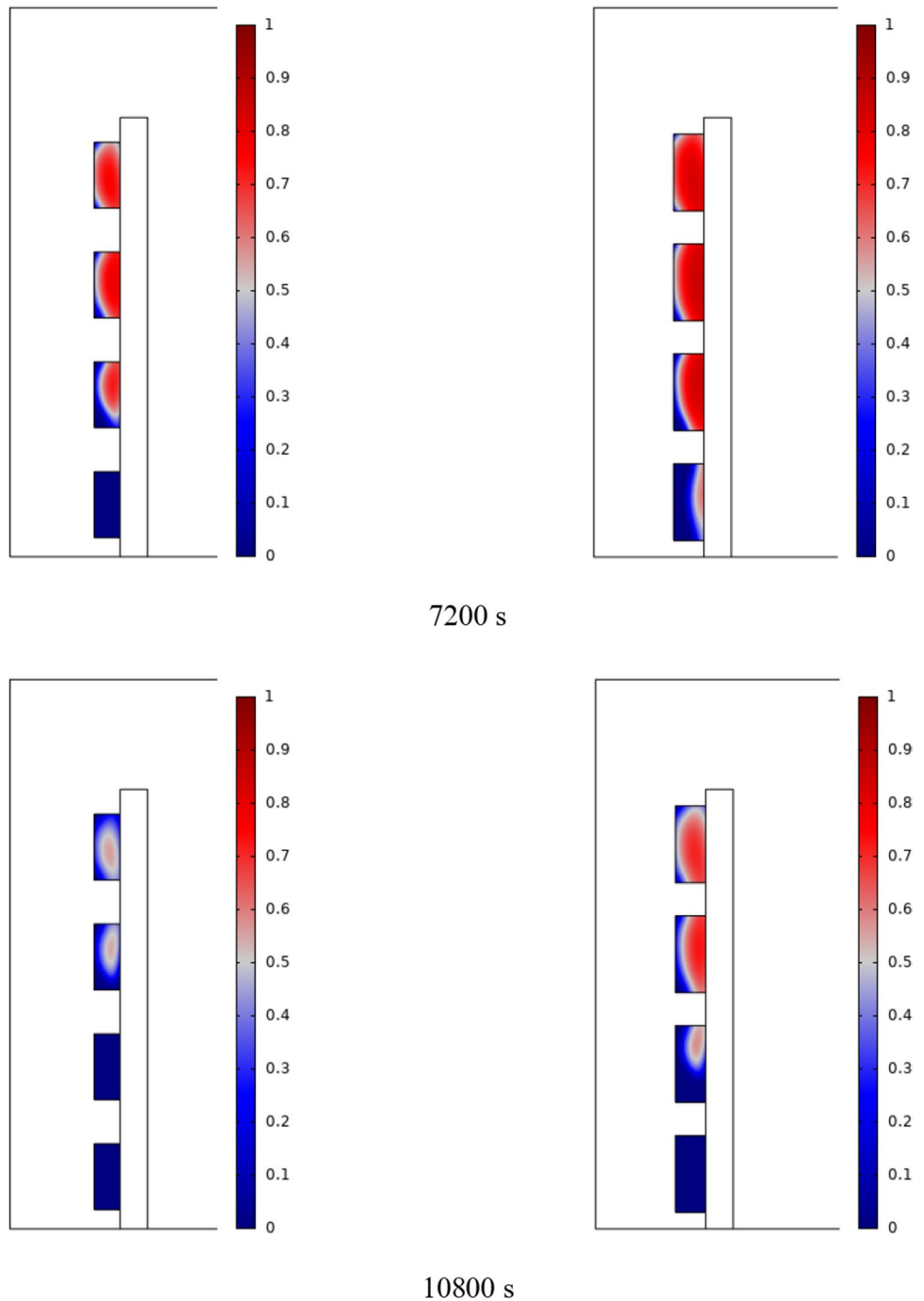
Fig. 7 (continued)



heat capacity. The energy formerly stored in the PCM during the day could be released into the atmosphere at night, leaving the exhaust TAR over the wall. During the phase transition, the PCM holds onto a significant

amount of energy in the form of latent heat of fusion. This energy is transferred to the air as latent heat over the night while turning molten PCM into solid PCM, increasing the TAR in front of the wall. In actuality, heat

Fig. 7 (continued)

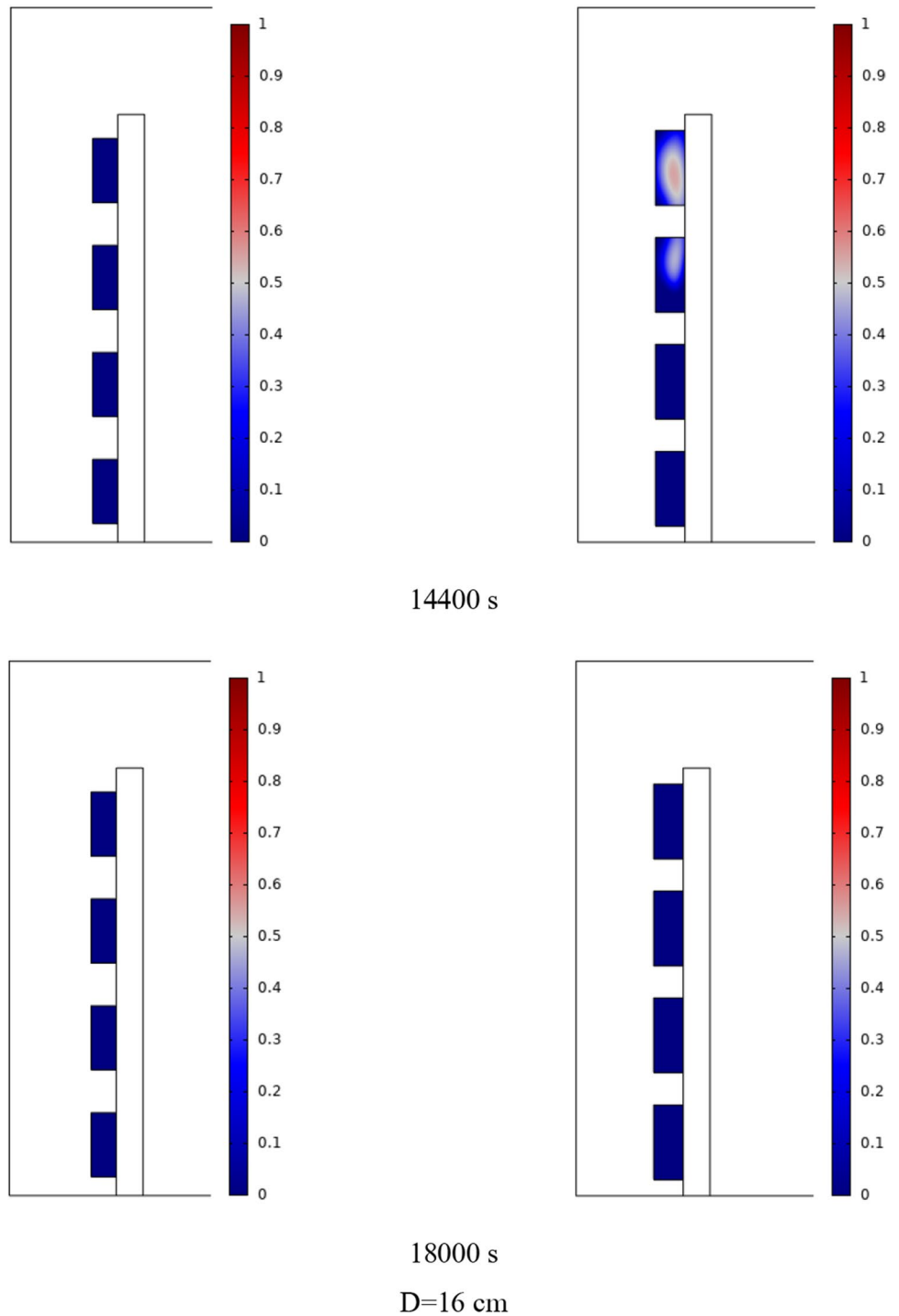


transfer from the PCM to the air takes longer the more PCM is used in the cavities.

The output TAR from the front of the Trombe wall at various (D)s from 8 to 16 cm from 0 to 7 h is shown in Fig. 9 for RECs. By creating airflow from the front of the wall, some of the latent energy in the PCM is transferred

to the air, raising the TAR. Over time, some of the PCM on the barrier's outside solidifies. When the PCM's outer shell hardens, there is a little reduction in the heat transfer from the liquid PCM to the air. The amount of TAR has decreased with time yet the PCM cavities have not stopped melting. The latent energy in the wall is released

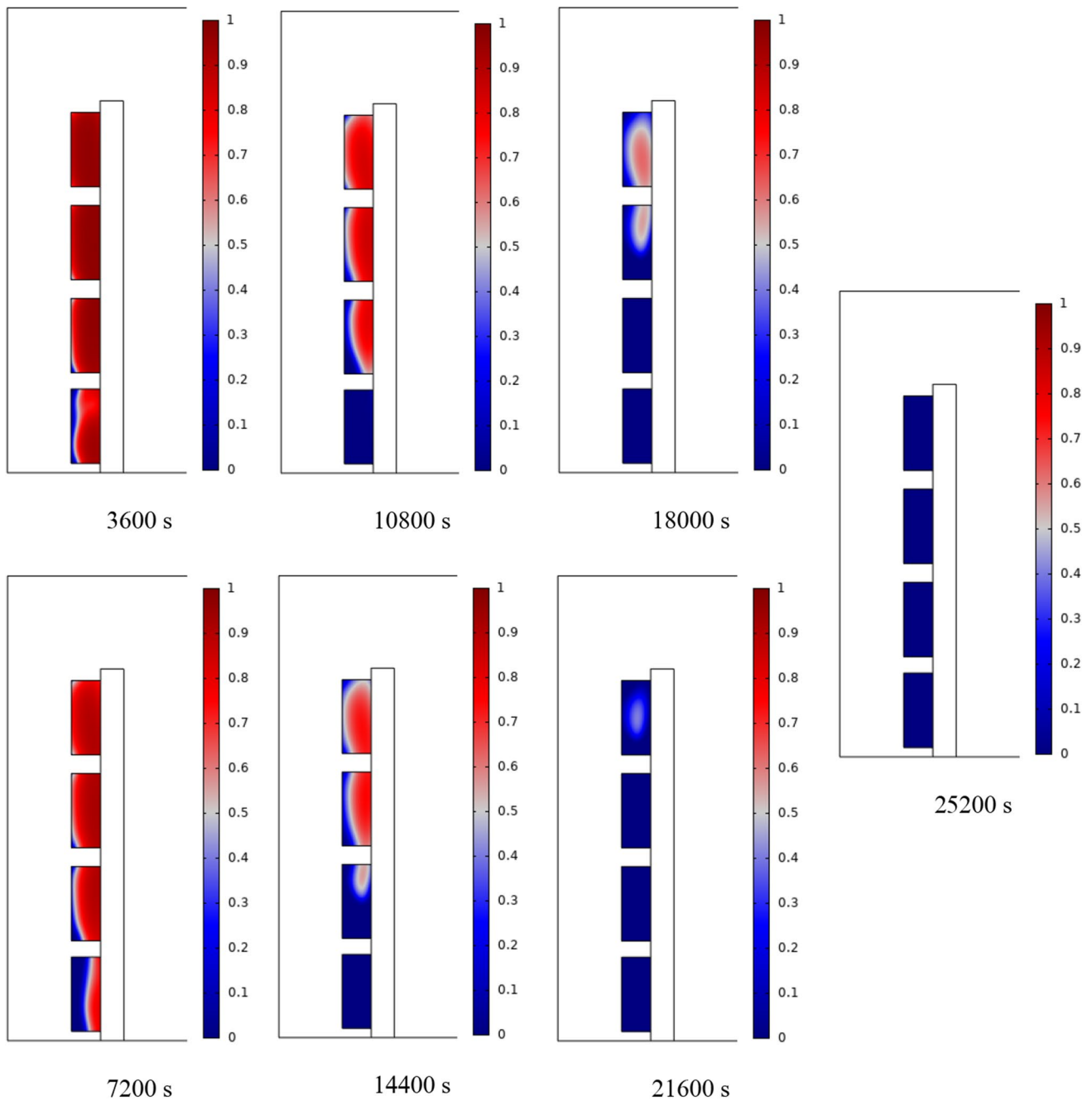
Fig. 7 (continued)



when the amount of molten PCM in the cavities becomes zero, and the TWL rapidly decreases. During this time, the temperature of the wall's exhaust air has been gradually dropping. More PCM being consumed in the wall allows the PCM to stay molten there for longer, which

causes the exhaust air coming from the front of the wall to be hotter for longer. The TAR is greater at fixed times due to the employment of an SEC on the wall as opposed to a REC. As compared to the wall with RECs, the wall with SECs had a higher outlet TAR over a longer length

Fig. 7 (continued)



of time. The usage of SECs has a more significant impact on the exit temperature of the wall, especially when the cavity dimensions are bigger.

As shown in Fig. 10, the Trombe TWL in different (D)s, from 8 to 16 cm, is shown from 0 to 7 h for SECs. This diagram shows the TWL along with the cavities.

If a conventional wall was used in a short time, its temperature would decrease in the absence of solar, but due to the use of PCM on the wall, the TWL remained high for a longer time due to the volume of PCM used. The heat stored in the PCM due to the sun's radiation during the night causes the TWL to remain at an acceptable

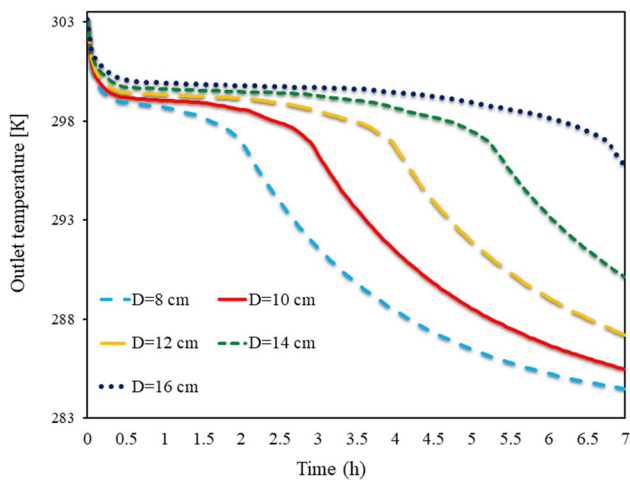


**Fig. 8** Exhaust TAR in front of the Trombe wall, in different (D)s from 8 to 16 cm, from 0 to 7 h for SECs

value and can also heat the room. Using more PCM on the wall also saves more energy on the wall. In this way, the wall can maintain its temperature for a longer time. So, in the aspect ratio of 16, the TWL at all times has been higher than other aspect ratios of obstacles, so that in the aspect ratio of 16 cm, the temperature has been above 295.5 for 7 h.

Figure 11 depicts the Trombe TWL at different (D)s from 8 to 16 cm from 0 to 7 h for RECs. The TWL is highly dependent on the PCM temperature inside the cavities. It is this latent energy in PCMs that allows the wall to maintain its high temperature for a long time. Therefore, in walls with obstacles with a larger aspect ratio, both the TWL is higher, and the TWL remains high for a longer time. By comparing the placement of REC and circular obstacles on the wall, it can be seen that using SEC causes the TWL to remain high for a longer time. Also, the TWL at constant times for the wall with SECs is higher than the wall with RECs, so that in 7 h at a 16 cm aspect ratio, the use of SECs causes the TWL to reach 2.1 °C higher than the wall with RECs.

In Fig. 12, in all SECs, the volume percentage of molten PCM is shown in various Ds ranging from 8 to 16 cm from 0 to 7 h. As long as thermal energy enters the PCM from outside the wall, the PCM remains molten. However, when the heat flux is cut off from outside the wall, the PCM freezing process begins

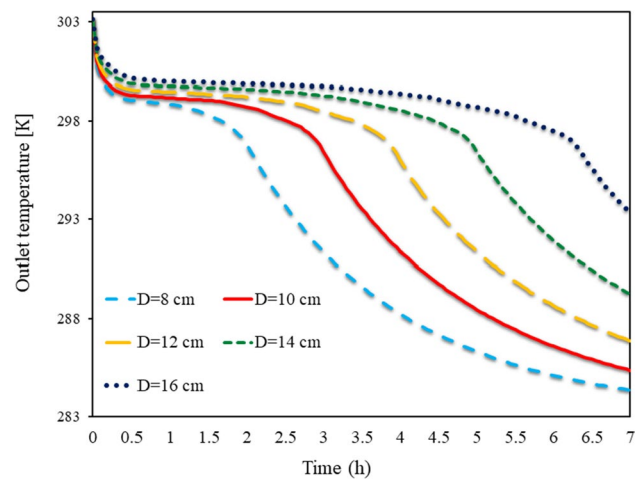


**Fig. 9** Exhaust TAR from the front of the Trombe wall in different (D)s from 8 to 16 cm from 0 to 7 h for RECs

due to the collision of cold air with obstacles. The process starts from the outer shell of the barrier and goes inside the barrier. Lower cavities freeze faster than upper cavities. By studying the average volume fraction of PCM, it can be seen that in smaller obstacles, due to the smaller volume of PCM, the whole PCM is frozen in less time. At constant periods, it can be shown that the quantity of molten PCM was greater when barriers with a bigger aspect ratio were employed. All PCMs in cavities with an 8 cm aspect ratio completely froze in a little under 2 h, but cavities with a 16 cm aspect ratio required more than 6.5 h to do the same.

In Fig. 13, the volume fraction of molten PCM is depicted on average in all RECs at different (D)s from 8 to 16 cm from 0 to 7 h. The air absorbs the latent energy inside the PCM, which causes the TAR to rise and the PCM to solidify inside the cavities. Smaller cavities on the wall have less PCM and therefore freeze entirely in less time. However, larger cavities require more time for the entire PCM to solidify. Comparing the two RECs and SECs, it can be seen that the time required for PCM solidification within cavities was longer for SECs than for RECs. Especially at higher aspect ratios, the increase in PCM freezing time was more dramatic. The time required for PCM solidification at a 16 cm aspect ratio in semi-circular obstacles was 15 min longer than in RECs.

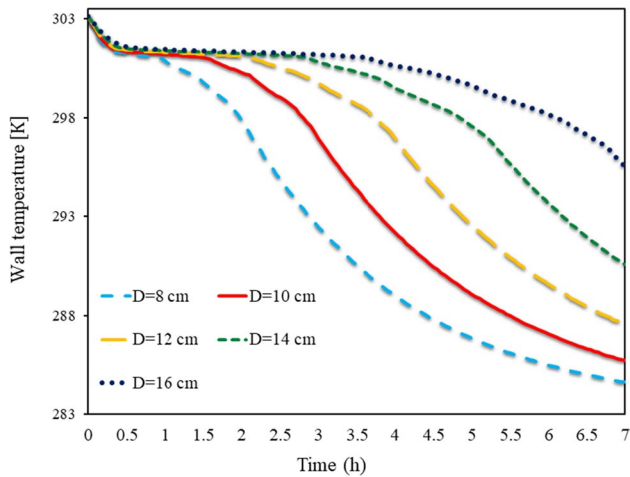


**Fig. 10** Trombe TWL in different (D)s, from 8 to 16 cm, from 0 to 7 h for SECs

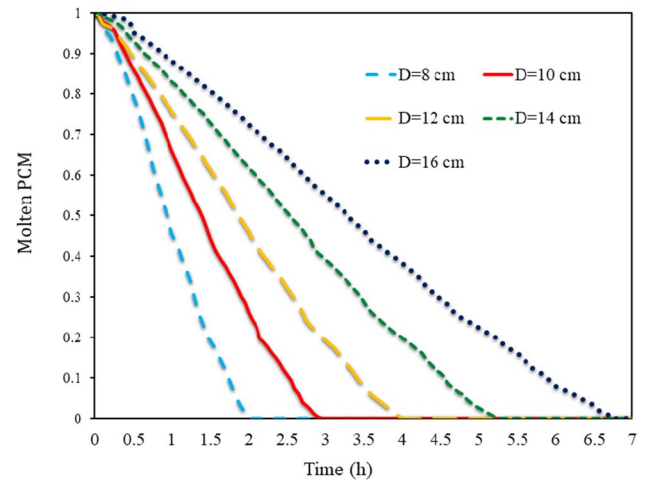


**Fig. 12** Volume fraction of molten PCM on average in all SECs at different (D)s from 8 to 16 cm from 0 to 7 h

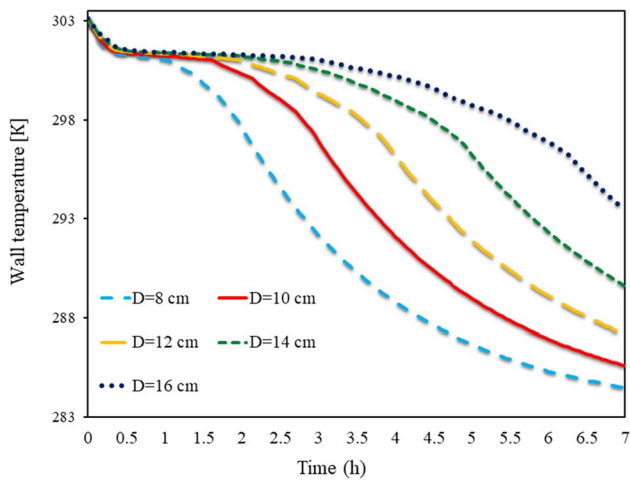


**Fig. 11** Trombe TWL in different (D)s from 8 to 16 cm from 0 to 7 h for RECs

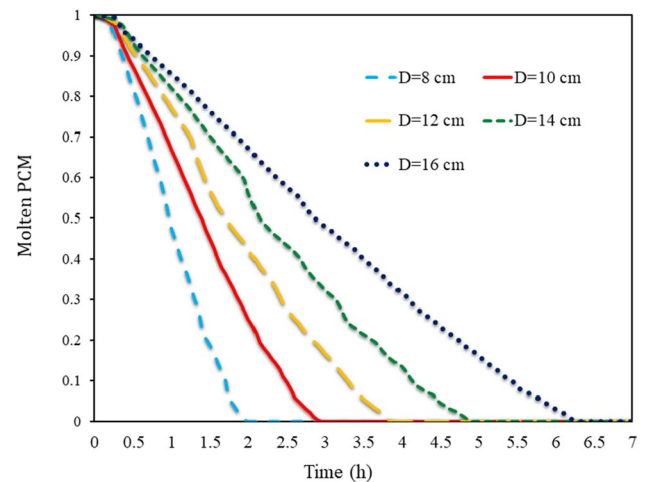


**Fig. 13** Volume fraction of molten PCM on average in all RECs in different (D)s from 8 to 16 cm from 0 to 7 h

## Conclusion

In this paper, the effect of using two types of SEC and RECs filled with PCM on a Trombe wall on the TWL, the complete freezing time of PCM, and the TAR leaving the wall have been numerically analyzed. Also, TWL contours and PCM solidification front progress in cavities have been studied. The outcomes of this investigation, which was conducted for 5 various cavity dimensions, are as follows:

(1) In general, the time required for PCM solidification in SECs is more than in RECs. However, in most cases, the time required to freeze the PCM at a 16 cm aspect ratio was 15 min longer in SECs than in RECs.

- (2) The TWL at constant times for the wall with SECs is higher than the wall with RECs, so that in 7 h at a 16 cm aspect ratio, the use of SECs causes the TWL to be 2.1 °C higher than the wall with RECs.
- (3) In the aspect ratio of 16, the TWL was higher than the other aspect ratios of the obstacles at all times, so that in the SEC, in the aspect ratio of 16 cm, after 7 h, the temperature was above 295.5.
- (4) For a longer time than the wall with RECs, the wall with SECs had a higher TAR. Especially in larger dimensions of cavities, the use of SECs has a better effect on the exit temperature of the wall.

**Author contribution** JM and SA performed the literature review, modelling, theoretical framework, and paper drafting. SH, BJ, FAA, and MS have performed an extensive analysis of the draft and developed the simulation models and editing. JM, SH, SA, FAA, and BJ contributed to the critical revision of the work. All authors have read and agreed to the published version of the manuscript.

**Funding** Open access funding provided by University of Pretoria. The authors are thankful to the Deanship of Scientific Research at Najran University for funding this work under the Research Priorities and Najran Research funding program grant code (NU/NRP/SERC/12/25).

**Data availability** Not applicable.

## Declarations

**Ethical approval** Not applicable.

**Consent to participate** Not applicable.

**Consent for publication** Not applicable.

**Competing interests** The authors declare no competing interests.

**Open Access** This article is licensed under a Creative Commons Attribution 4.0 International License, which permits use, sharing, adaptation, distribution and reproduction in any medium or format, as long as you give appropriate credit to the original author(s) and the source, provide a link to the Creative Commons licence, and indicate if changes were made. The images or other third party material in this article are included in the article's Creative Commons licence, unless indicated otherwise in a credit line to the material. If material is not included in the article's Creative Commons licence and your intended use is not permitted by statutory regulation or exceeds the permitted use, you will need to obtain permission directly from the copyright holder. To view a copy of this licence, visit <http://creativecommons.org/licenses/by/4.0/>.

## References

- Aberoumand S, Ghamari S, Shabani B (2018) Energy and exergy analysis of a photovoltaic thermal (PV/T) system using nanofluids: an experimental study. *Solar Energy* 165:167–177
- Aghakhani S, Afrand M (2022) Experimental study of the effect of simultaneous application of the air- and water-cooled flow on efficiency in a photovoltaic thermal solar collector with porous plates. *Appl Therm Eng* 217:119161
- Aghakhani S, Ghaffarkhah A, Arjmand M, Karimi N, Afrand M (2022) Phase change materials: agents towards energy performance improvement in inclined, vertical, and horizontal walls of residential buildings. *J Build Eng* 56:104656
- Al-Abidi AA, Mat S, Sopian K, Sulaiman MY, Mohammad AT (2014) Experimental study of melting and solidification of PCM in a triplex tube heat exchanger with fins. *Energy and Build* 68:33–41
- Amjad M, Jin H, Du X, Wen D (2018) Experimental photothermal performance of nanofluids under concentrated solar flux. *Sol Energy Mater Sol Cells* 182:255–262
- Arasu AV, Mujumdar AS (2012) Numerical study on melting of paraffin wax with Al<sub>2</sub>O<sub>3</sub> in a square enclosure. *Int Commun Heat Mass Transf* 39(1):8–16
- Ascione F, Bianco N, Iovane T, Mastellone M, Mauro GM (2021) The evolution of building energy retrofit via double-skin and responsive façades: a review. *Solar Energy* 224:703–717
- Barbosa S, Ip K (2014) Perspectives of double skin façades for naturally ventilated buildings: a review. *Renewable Sustainable Energy Rev* 40:1019–1029
- Bellos E, Tzivanidis Z, Zisopoulou E, Mitsopoulos G, Antonopoulos KA (2016) An innovative Trombe wall as a passive heating system for a building in Athens—a comparison with the conventional Trombe wall and the insulated wall. *Energy Build* 133:754–769
- Biwole PH, Eclache P, Kuznik F (2013) Phase-change materials to improve solar panel's performance. *Energy Build* 62:59–67
- Bojić M, Johannes K, Kuznik F (2014) Optimizing energy and environmental performance of passive Trombe wall. *Energy Build* 70:279–286
- Bouhal T, Fertahi S e-D, Kousksou T, Jamil A (2018) CFD thermal energy storage enhancement of PCM filling a cylindrical cavity equipped with submerged heating sources. *J Energy Storage* 18:360–370
- Elghamry R, Hassan H (2020) Experimental investigation of building heating and ventilation by using Trombe wall coupled with renewable energy system under semi-arid climate conditions. *Solar Energy* 201:63–74
- Hu Z, He W, Ji J, Zhang S (2017) A review on the application of Trombe wall system in buildings. *Renewable Sustainable Energy Rev* 70:976–987
- Izadi M, El Haj Assad M (2021) Chapter 15 - use of nanofluids in solar energy systems. In: Assad MEH, Rosen MA (eds) *Design and Performance Optimization of Renewable Energy Systems*. Academic Press, pp 221–250
- Jamil F, Ali HM, Janjua MM (2021) MXene based advanced materials for thermal energy storage: a recent review. *J Energy Storage* 35:102322
- Kara YA, Kurnuç A (2012) Performance of coupled novel triple glass and phase change material wall in the heating season: an experimental study. *Solar Energy* 86(9):2432–2442
- Karthick K, Suresh S, Hussain MMMD, Ali HM, Kumar CSS (2019) Evaluation of solar thermal system configurations for thermoelectric generator applications: a critical review. *Solar Energy* 188:111–142
- Khetib Y, Alotaibi AA, Alshahri AH, Cheraghan G, Sharifpur M, Meyer JP (2021) Study on the effect of hole size of trombe wall in the presence of phase change material for different times of a day in winter and summer. *Processes* 9:1886
- Lawag RA, Ali HM (2022) Phase change materials for thermal management and energy storage: a review. *J Energy Storage* 55:105602
- Lin K, Zhang Y, Xu X, Di H, Yang R, Qin P (2005) Experimental study of under-floor electric heating system with shape-stabilized PCM plates. *Energy Build* 37(3):215–220
- Mahdi JM, Lohrasbi S, Ganji DD, Nsofor EC (2019) Simultaneous energy storage and recovery in the triplex-tube heat exchanger with PCM, copper fins and Al<sub>2</sub>O<sub>3</sub> nanoparticles. *Energy Convers Manag* 180:949–961
- Mustafa J, Alqaed S, Kalbasi R (2021) Challenging of using CuO nanoparticles in a flat plate solar collector- energy saving in a solar-assisted hot process stream. *J Taiwan Inst Chem Eng* 124:258–265
- Oluah CK, Akinlabi ET, Njoku HO, Jen TC (2021) Development of software codes and system architecture for optimum performance Trombe wall system in buildings using IoT devices. *Mater Today Proc* 44:1185–1189
- Omrany H, Ghaffarianhoseini A, Ghaffarianhoseini A, Raahemifar K, Tookey J (2016) Application of passive wall systems for improving the energy efficiency in buildings: a comprehensive review. *Renewable Sustainable Energy Rev* 62:1252–1269
- Parsa SM, Yazdani A, Javadi D, Afrand M, Karimi N, Ali HM (2022) Selecting efficient side of thermoelectric in pyramid-shape solar desalination units incorporated phase change material (PCM), nanoparticle, turbulator with battery storage powered by photovoltaic. *J Energy Storage* 51:104448

- Saadatian O, Sopian K, Lim CH, Asim N, Sulaiman MY (2012) Trombe walls: a review of opportunities and challenges in research and development. *Renewable Sustainable Energy Rev* 16(8):6340–6351
- Sergei K, Shen C, Jiang Y (2020) A review of the current work potential of a trombe wall. *Renewable Sustainable Energy Rev* 130:109947
- Tlili I, Alharbi T (2022) Investigation into the effect of changing the size of the air quality and stream to the trombe wall for two different arrangements of rectangular blocks of phase change material in this wall. *J Build Eng* 52:104328
- Usman M, Ali M, ur Rashid T, Ali HM, Frey G (2021) Towards zero energy solar households – a model-based simulation and optimization analysis for a humid subtropical climate. *Sustain Energy Technol Assess* 48:101574
- Xiong Q, Altnji S, Tayebi T, Izadi M, Hajjar A, Sundén B, Li LKB (2021) A comprehensive review on the application of hybrid nanofluids in solar energy collectors. *Sustain Energy Technol Assess* 47:101341
- Yang M, Wang E-Z, Hou Y (2021) The relationship between manufacturing growth and CO<sub>2</sub> emissions: does renewable energy consumption matter? *Energy* 232:121032
- Yang X-H, Tan S-C, Liu J (2016) Numerical investigation of the phase change process of low melting point metal. *Int J Heat Mass Transf* 100:899–907
- Zalewski L, Joulin A, Lassue S, Dutil Y, Rousse D (2012) Experimental study of small-scale solar wall integrating phase change material. *Solar Energy* 86(1):208–219
- Zhou G, He J (2015) Thermal performance of a radiant floor heating system with different heat storage materials and heating pipes. *Appl Energy* 138:648–660

**Publisher's note** Springer Nature remains neutral with regard to jurisdictional claims in published maps and institutional affiliations.